# Role of free volume on the mechanical properties of Cu-Zr based metallic glasses: A molecular dynamic study

A thesis submitted in partial fulfillment of the

requirements for the degree of

**Master of Technology**

**In**

**Metallurgical and Materials Engineering**

**By**

**Amarjyoti Kabi**
**(Roll No-213MM1469)**


Department of Metallurgical and Materials Engineering
National Institute Of Technology,
Rourkela-769008, Odisha, India
May-2015.

# Role of free volume on the mechanical properties of Cu-Zr based metallic glasses: A molecular dynamic study

A thesis submitted in partial fulfillment of the

requirements for the degree of

**Master of Technology**

**In**

**Metallurgical and Materials Engineering**

**By**

**Amarjyoti Kabi**
**(Roll No-213MM1469)**

Under the guidance and supervision of

**Prof. Natraj Yedla**


Department of Metallurgical and Materials Engineering
National Institute Of Technology
Rourkela-769008, Odisha, India
May-2015.


**DEPARTMENT OF METALLURGICAL & MATERIALS ENGINEERING**

**NATIONAL INSTITUTE OF TECHNOLOGY, ROURKELA**

# Certificate

This is to certify that the Project Report entitled "**Role of free volume on mechanical properties of Cu-Zr based metallic glasses-A molecular dynamics study**", submitted by **Mr. Amarjyoti Kabi (213mm1469)**, in partial fulfilments for the needs for the award of **Master of Technology** Degree in **Metallurgical & Materials Engineering** at **National Institute of Technology, Rourkela,**is an authentic work executed by him under my direction and guidance. To the best of my awareness, the substance embodied in the report has not been submitted to any other University / Institute for the award of any Degree.

**Date:**28th May,2015

**Prof. Natraj Yedla**

Assistant Professor
Department of Metallurgical & Materials Engineering
National Institute of Technology, Rourkela

# ACKNOWLEDGEMENT

I would like to show gratitude to **NIT Rourkela** for giving me the prospect to utilize its assets and work in such an exigent environment. First and foremost, I take this chance to articulate my profound regards and honest gratefulness to my guide **Prof. N. Yedla** for his proficient supervision and invariable support throughout my project work. This project would not have been achievable without his aid and the priceless time that he has given me amidst his tiring schedule.

I would also like to express my paramount gratitude to **Prof. S.C Mishra, HOD, Metallurgical & Materials engineering** for permitting me to use the departmental amenities.

I would also like to extend my jovial gratefulness to my associates and superior students of this branch who always encouraged and supported me in undertaking my work. Last but not the least; I would like to thank all the employees of Department of Metallurgical &Materials Engineering who were incredibly cooperative with me.

**Amarjyoti Kabi**

**(213mm1469)**

**Metallurgical & Materials Engineering**

**National Institute of Technology, Rourkela**

# ABSTRACT

In this thesis the investigation is being carried out on mechanical properties of $Cu_{50}$-$Zr_{50}$ based metallic glass obtained at different cooling rates using Molecular Dynamics (MD) simulation techniques. Metallic glasses or an amorphous material has pulled in extensive consideration because of their remarkable mechanical properties such as better strength, wear, corrosion resistance and it is twice as solid as titanium. And it is harder and more flexible than ceramics. Because of their enhanced properties over crystalline metals have made them adaptable engineering material for many engineering applications..All the MD simulations are coded in LAMMPS. A box of dimension 50 × 100 × 50 $Å^3$containing 21952 number of atoms of $Cu_{50}$-$Zr_{50}$are created and then the crystalline alloy is quenched at different cooling rates ($10^{11}$K/s-$10^{14}$ K/s). The different cooling rates induce different free volume content and are found to have a significant effect on the mechanical properties. With increasing cooling rate the free volume of the material increases. With higher free volume material will extend effortlessly under low stress. The samples are then subjected to uniaxial tensile and compressive deformation at different strain rates and at temperatures (300K, 200K, 100K, 50K and 10K). The effect of strain rates, temperatures and excess free volume of the mechanical properties such as yield strength, young's modulus and ultimate tensile strength is investigated from the stress-strain plots. Inter atomic forces are calculated by using the embedded atom method (EAM). The changes in the atomic structure and deformation can be observed with the help of Ovito snap shots. It is found that strength increases with increase in strain rates and decrease of temperatures.

Keywords: Metallic glass, Molecular dynamics, LAMMPS, Strain rate.

# Table of Contents

# List of Figures

# List of Tables

# CHAPTER-1

# INTRODUCTION

## 1.1Background

At the present time, irresistible advancement of science and innovation has preparedfor researchers to discover new materials for high innovation applications. The materials utilized for innovative applications are intended to have most extreme execution at ideal conditions. Some of the contemporary engineering materials which have pulled in extensive consideration of material researchers are shape memory alloys (SMA), carbon nanotubes, nanophase materials,metallic glasses and so on. Here the motivation of the project work is on the Metallic Glasses.

A glass is nothing but the any material that can be cooled from a liquid to a solid without crystallization. Most metals do take shape as they cool, organizing their atoms into aexceptionally consistent spatial called a lattice. If by in any case crystallization can be halted or does not happen, and the particles subside into an almost irregular course of action, the last shape is called metallic glass.

So metallic glass, also known as glassy metal was first discovered by Pol Duwez in the year of 1960 at California Institute of Technology[1]. Metallic glasses are strong composites that are non-crystalline structure, having a nuclear course of action acquired straightforwardly from the liquid state.They utilized the process of fast extinguishing procedures for cooling the fluid metals at extremely high rates approximate 10°C per second.Due to high cooling rates the atoms are not arranged in perfect manner for which it gives glassy or amorphous structure which is shown in Fig.1.1(a) and in crystalline material, atoms are arranged in regular pattern which is shown in Fig. 1.1(b).

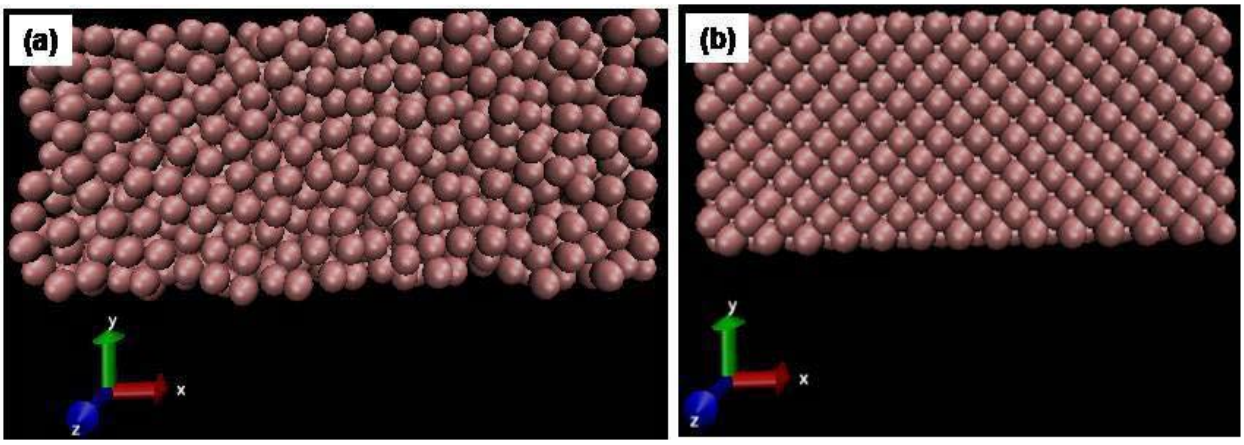


Fig.1.1: atomic arrangement of (a) glassy structure (b) crystalline structure.

Due to absence of long range order, metallic glasses have selective mechanical properties which make them keen materials for creating segments for scope of uses in different engineering applications. Also it seems to have a brilliant future as it is twice as solid as titanium, harder and more flexible than ceramics and having superb wear and corrosion resistance makes them appealing for a mixed bag of uses as compared to other conventional materials. In spite of their high quality contrasted with crystalline materials, display poor ductility. General deformation classification of Cu-Zr based metallic glasses; both in tensile and compressive mode have been done to investigate the likelihood of room temperature pliability in these metallic glasses[2-5].As indicated by a few analysts, ductility of metallic glass increases due to presence of crystalline phase[6].Couple of studies state that, the presence of crystalline phase decreases the ductility of metallic glass [7]. It has been shown that addition of Ti to Cu-Zr metallic glass promotes crystallization and increases the plasticity[8]. Also addition of Al to Cu-Zr metallic glass enhance the ductility[9, 10].

## 1.2 Production Techniques

To produce metallic glass rapid quenching rate is required. There are several rapid quenching techniques are listed below:

**Liquid Quenching:**

In this technique, a little fluid globule was pushed into little drops by with the help of a shock tube and the drops were splashed into thin foil on a copper substrate. Quenched samples can be produced in irregular shape with altering thickness from about 1pmto 10 pm.

**Atomic Condensation:**

In this system,profoundly disordered structure is attained to by bringing down the mobility of the atoms so that atoms concentrate without crystallization. vapour condensation at liquid helium temperature has yielded high superconducting amorphous films of Ga, As, Sb, Bi and Ga.

**Atomization and Chilling Methods:**

Atomization method includes discontinuity or atomization of the melt stream into fine droplets but chilling method includes solidification of melt stream[11]. Fig.1.2: shows the rapid solidification of atomization and chilling processes.

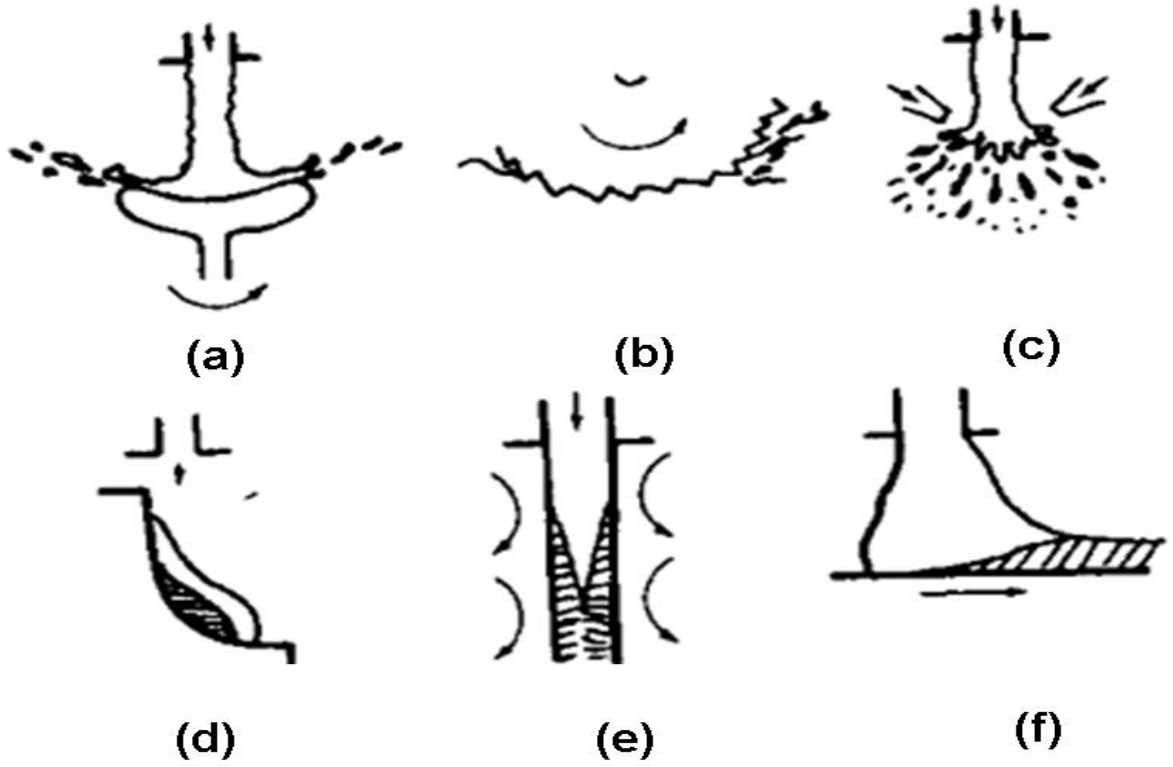


Fig.1.2: (a,band c) shows the atomization method and (c,d and e) shows the chilling methods.

# 1.3 Classification of metallic glasses

Metallic glasses are generallyclassified under two categories:

1. **Metal-Metal metallic glasses:**

   It consists of metals only. It can be classified into four sub-categories (a) rare-earth metals (b) transition metals (c) uranium, neptunium or plutonium (d) alkali metals. Examples of metal-metal metallic glasses are Cu-Zr, Mg-Zn, Ti-Ni etc.

2. **Metal-Metalloid metallic glasses**:

It mainly consists ofearly transition metals(Zr,Ti....), late Transition metals(Ni, Fe, Co....) and metalloid elements such as Si, C, B or P etc.

# 1.4 Properties

- In crystalline material, the thermal conductivity is higher than the amorphous material.
- Amorphous metals are less brittle and much tougher than ceramics and oxide glasses.
- High viscosity prevents the atoms affecting enough to outline an well-ordered lattice.
- Metallic glasses are very easily magnetized at low magnetic field strength.
- Metallic glasses have excellent wear and corrosion resistance and also posses unique mechanical and electrical properties.
- It shows poor ductility at room temperature and fails unexpectedly when the metals undergoes tension, which restricts their low temperature applications.

# 1.5 Applications

- Owing to malleable and ductility, they are utilized in filament windings.
- They carry on as superconductors thus they are utilized as a part of creation of high magnetic field.
- As a result of high electrical resistance they are utilized to make computer memories.
- Because of corrosion resistance they are utilized in marine vessels and surgical clips.
- Shot-peening balls.
- Casing in celluar phones.
- Casing in electro-magnetic instruments.
- Various shape of optical mirrors.
- Frame in tennis racket.
- Soft magnetic choke coils.
- High torque geared motor parts.

❖ Thin films of amorphous metals can be deposited via high velocity oxygen fuel technique as private coatings.

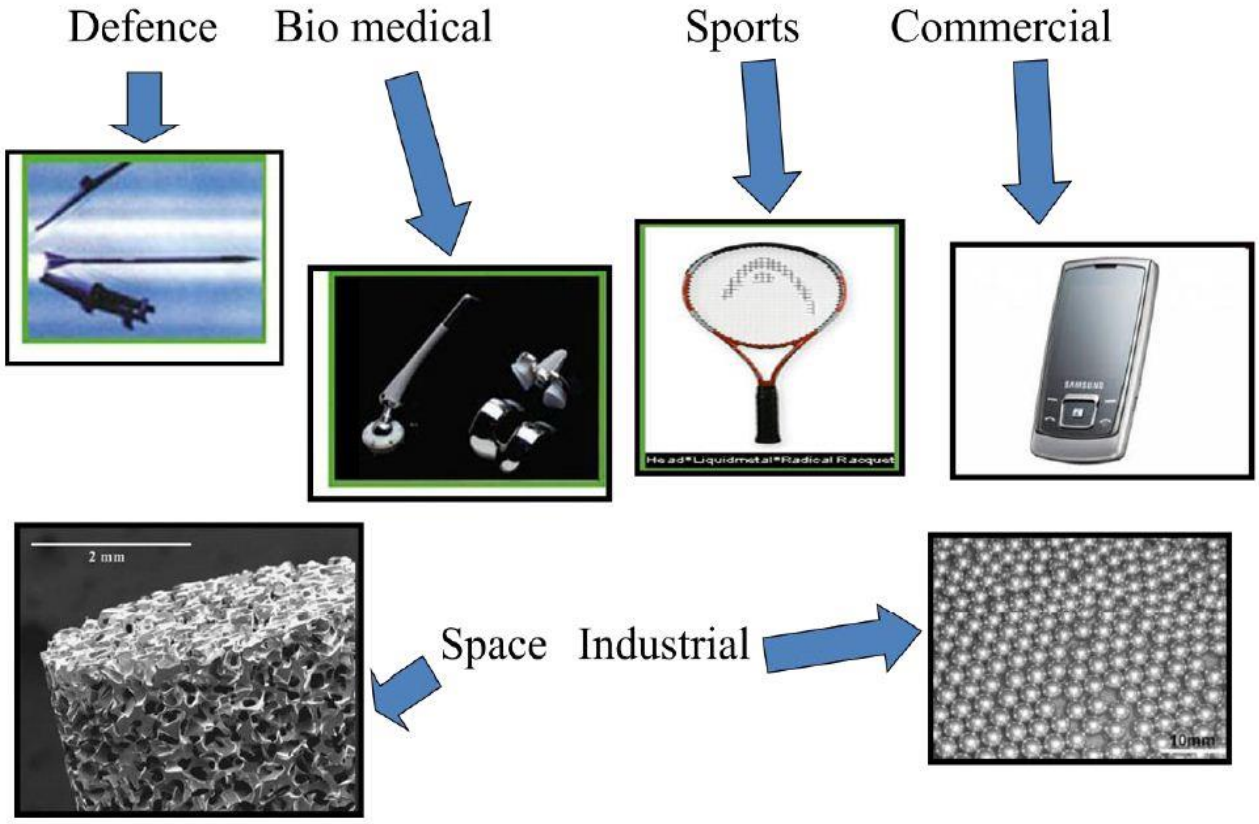


Fig. 1.3: Applications of metallic glasses.

## 1.6 Objectives of Research Work

(a) Calculation of excess free volume present in Cu-Zr metallic glasses induced due to different cooling rates in the range of $10^{10}$ K/s-$10^{14}$ K/s.

(b) To investigate the effect of different strain ratesin the range of $10^{9}s^{-1}$ - $10^{12}s^{-1}$ and temperatures (10K, 50 K, 100 K, 200 K, and 300 K)on the tensile deformation behavior of $Cu_{50}$-$Zr_{50}$ metallic glass.

(c) To investigate the effect of different strain rates in the range of $10^{8}s^{-1}$ - $10^{12}s^{-1}$ and temperatures (10K, 50 K, 100 K, 200 K, and 300 K) on the compressive deformation behavior of $Cu_{50}$-$Zr_{50}$ metallic glass.

# CHAPTER-2

# LITERATURE SURVEY

# 2 Literature Survey

## 2.1 Background

At the point while the liquid phase cooled to underneath its freezing temperature, changes into a solid phase called crystalline solid. But some liquid don't take shape due to complex atomic design or moderate sub-atomic transport, but as an alternativeforms a disordered structure well-known as glasses which is fundamentally the same structure to that of the liquid and consequently amorphous metals are frequently reffered to as “metallic glass” or “glassy metals”[12]. On the other hand there are numerous methods where amorphous metals can be formed such as physical vapour deposition(PVD), spray techniques, ion irradiation and sputtering[13]. In the dawn period amorphous metals have been formed by rapid quenching methods or mechanical amorphization as revealed in Fig. 2.1. Alloys showingfine glass-forming ability usually have a minute energy difference stuck between the amorphous and crystalline solid phases ($E_{ac}$) leads to a smaller driving force for crystallization.

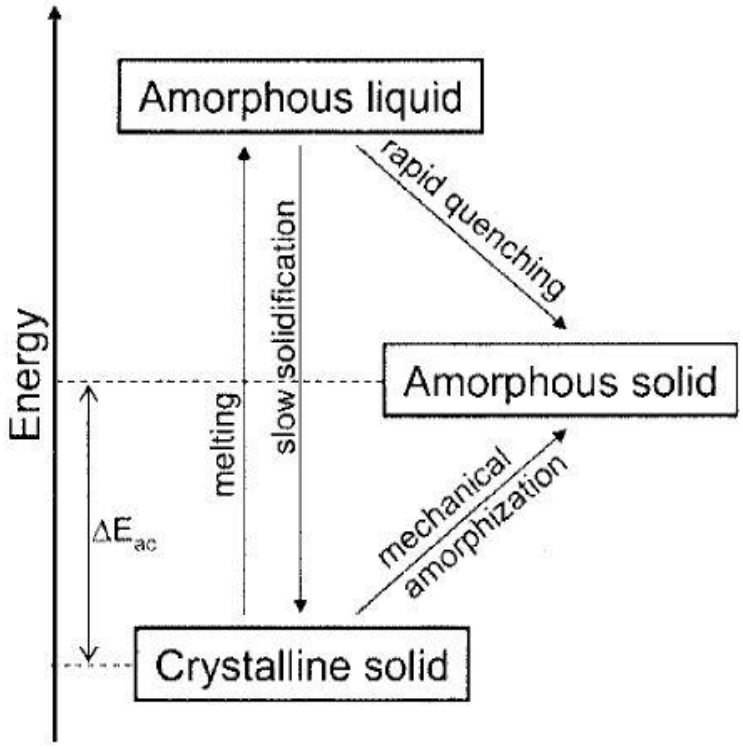


Fig. 2.1 Transformation of crystalline solid to amorphous solid and energy levels between them.

Since 1990 the restrictions of bulk metallic glass synthesis were rise above and some alloys with significant cooling rates (in the range of 1 K/s – 100 K/s) which are low enough to allow the formation of amorphous structure in thick layers (over 1 millimeter) have been produced[14,15]. These are familiar as bulk metallic glasses(BMGs). The glass forming abilityis the simplicity with which crystallization can be avoided and accordingly create a glassy state of material from rapid cooloing. So glasses are having disordered atomic configuration and the crystalline structure has ordered structure. Fig. 2.2 demonstrates the atomic arrangements in glassy structure and in crystalline structure.[16,17].

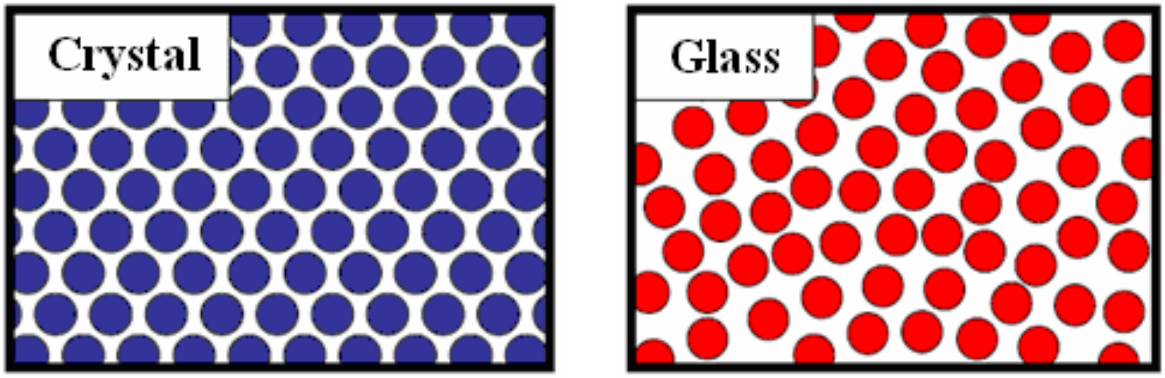


Fig. 2.2: Atomic arrangement of glassy and crystalline structure.

## 2.1.1Formation of glassy state

After cooling the liquid phase transforms into crystal or glass, depends upon the rate of cooling. If liquid phase undergoes a rapid cooling it forms a glassy state otherwise it forms a crystalline solid which is revealed in Fig. 2.3. Under cooling a liquid from beginning state A, the volume decreases consistently together with the path AB. If the cooling rate is slow and nucleation occurs, then crystallization occurs at freezing temperature($T_x$). Then volume decreases roughly from B to C, subsequently, the solid will deal with falling temperature along the way CD. The higher cooling rate restrain the nucleation for which crystallization does not occur at $T_x$ and thus the volume of the supercooled liquid decreases along the way BE. At point 'E'the volume–temperature graph undergoes a major change in slope and continues exactly parallel to the graph CD. $T_g$ is the temperature where glassy material changes to soft material.

$T_g$increases with cooling rate and therefore it is suitable to describe it a transformation range relatively than a fixed point. Below Tg the volume "V" decreases slowly to v′which issmooth prolongation of the contraction way BE of the supercooled liquidand represents undercooling. With increasing cooling rate the commencement of the glass transition increases[18,19].

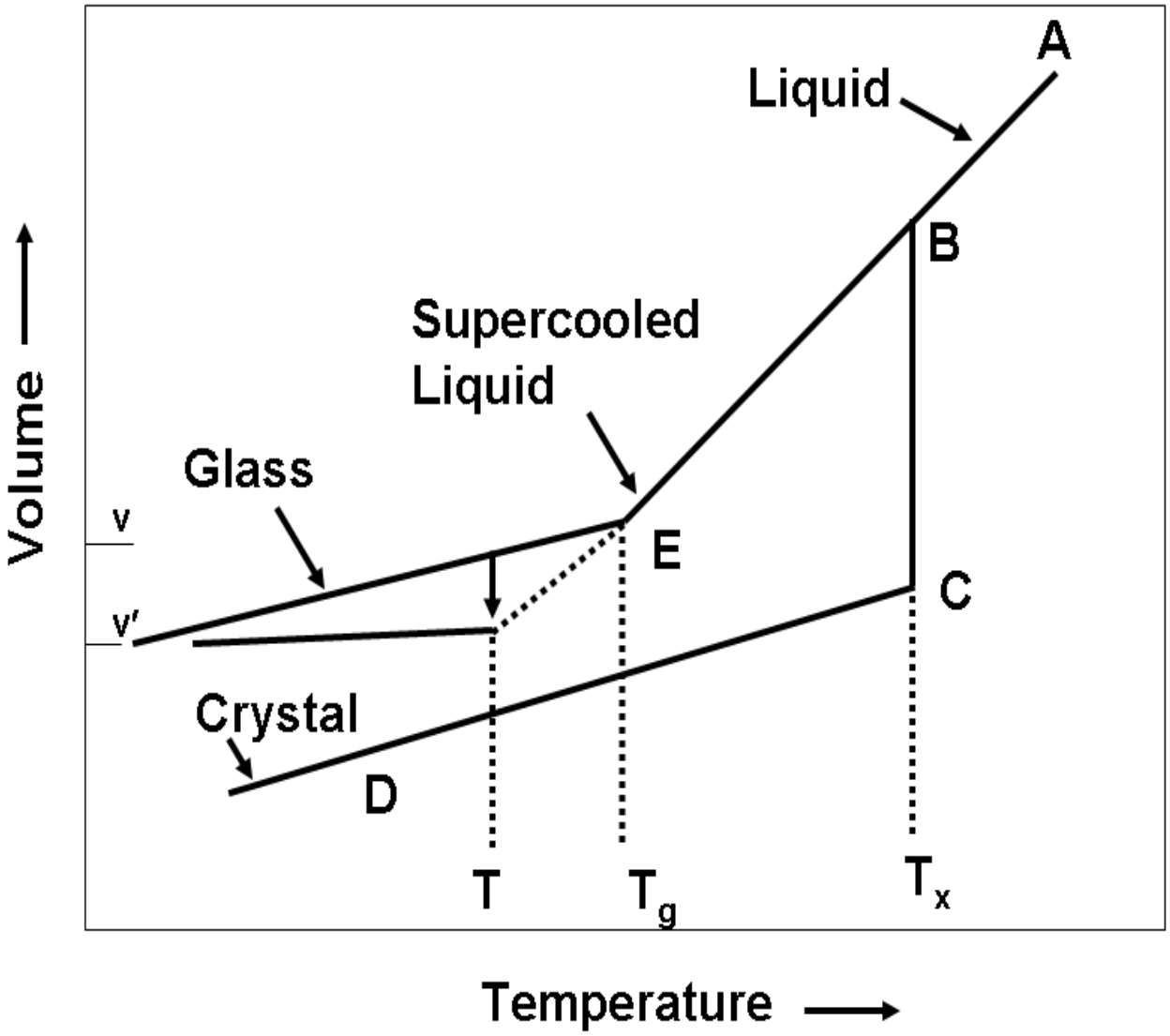


Fig. 2.3: Volume Vs Temperature plot among liquid, glassy and solid states

## 2.2 Metallic Glasses

With the assistance of rapid quenching methods such as electrodeposition, vapour condensation and chemical deposition the liquid composition can be taken for many metals and alloys[20]. Amorphous alloys represents the young set of materials which has been developed in 1960 by Klement et al. an experiment on Au-Si alloys [21]. BMGs have been produced in various multi-component alloys. Bulk metallic glasses are appropriate to structural materials, and their mechanical properties have turned into a matter ofenormousattention. Metallic glasses has variety of features which make them different from ceramic alloys, crystalline alloys and other kind of smart materials which are discussed below [21,22].

- Localized shear deformation: At room temperature, for the most part of inorganic glasses are brittle in nature and have a smooth fracture surface. Alternatively, metallic glasses are generally deformed at room temperature by localized shear deformation and moreover ductile in nature while rolling and bending deformation takes place. Under uniaxial tensile deformation metallic glasses are undergoes shear deformation after yield values without showing considerable microscopic plastic strain. Fig. 2.4 shows how the yield strength varies with respect to temperature under uniaxial tensile deformation.

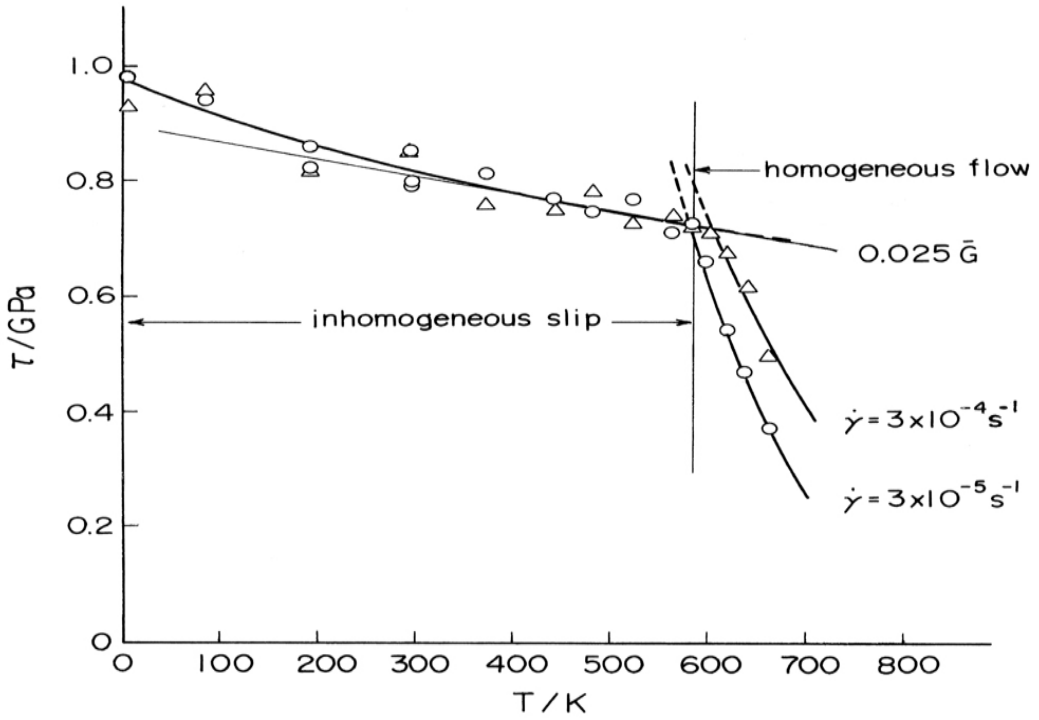


Fig.2.4: Yield strength Vs Temperature plot under tensile deformation

Metallic glass samples demonstrate homogeneous viscous flow at glass transition temperature and beyond critical temperature. Below critical temperature the metallic glass deforms plastically by localized shear deformation.

Even though metallic glasses are having attractive mechanical properties, failure and yielding mechanism is still not comprehensively understood.It is accounted for that at surrounding temperature the procedure of deformation of metallic glasses is "shear banding" where plastic strain is exceptionally limit into portions of nanometer thickness and macroscopic length.The execution of shear bands on the nanometer scale offers ascend to extraordinary mechanical properties at macroscopic scales.With respect to sample, the amorphous materials under low tensile value fails sharply along the shear band.These extraordinary properties have been seen in an assortment of glassy alloys with altered composition.BMGs have additionally pulled in due to large elastic limit. On the other hand, the room temperature weakness and strain-softening nature constrain their genuine structure applications. Among numerous thoughts and their execution was to be done to triumph over this issue, creating BMG-matrix composite has useful compressive plasticity and toughness[23]. By fitting altering dendrite dividing through controlling preparation route tensile ductility has been absorbed by Johnson et al.[24,25]. They were accomplishing tensile ductility in Zr and Ti based BMG composites. But even after this investigation, BMG composite experience strain softening with neckingoccurs near yield point because of lack of work-hardening mechanism. For industrial applications, work-hardening capacity and homogeneous tensile ductility are necessary, therefore addition of ternary elements such as Ti,Al, Ag to Cu-Zr-based alloy improve the glass forming ability drastically.In Cu-Zr system, intermetallic compound with an austenite or martensite like structure enhances their plasticity; however the mechanism of deformation of martensitic stage amid tensile loading is still uncertain[26]. A trademark highlight of plastic deformation of metallic glasses at the ambient temperature is the localized shear deformation.. Since we have no fitting test system, dissimilar to crystalline matter, to approach minute deformation prepare in formless materials, we need to confidence on computer simulation examines by utilization of atomistic models to uncover the infinitesimal distortion forms.

## 2.3 Deformation mechanism of metallic glasses

It is surely understood that the mechanical properties of crystalline materialsdepends upon on the crystal structure and the plasticdeformation is occurred by twins, dislocation and diffusive development however in glass because of the disordered atomic structure the deformation system is distinctive to that of crystalline materials, i.e., the plastic deformation is not interceded by dislocations and twins, which are vague.Even if lacking long range-order, metallic glasses possess short range ordering as proposed by the several atomic packing models[27-29]. Inspite of the atomic packing, the total volume of the amorphous material can be shared into, space employed by the atomic clusters and the free space between the clusters. The free space is called as free volume and around it atoms have lower nuclear coordination in respect to those inside of the atomic clusters[30,31]. In metallic glasses strains are produced because of shear transformations nucleated as a result of applied stress and also because of thermal instabilities which takes place nearby the positions of free volume of the amorphous structure. With the assistance of two hypothetical models: one based on spaepen free-volume and other is Argon shear transformation zone(STZ), described the deformation behaviour of metallic glasses[32,33]. Fig.2.5(a) illustrates the behaviour of plastic fow in amorphous materials or metallic glasses while Fig.2.5(b) illustrates the free volume model, established by Turnbull et al.[34] it shows how an atom jumps from one place to another.This occurrence is termed as "flow" imperfection or "neighborhood inelastic movement" and progressively generally a "shear transformation zone (STZ). The STZ comprise of group of atoms which is reason for inelastic shear alteration from low energy arrangement to high energy arrangement.

According to Argons model, the flow can confine in a group wherein strain rate has been diverted, while the applying stress work the confined shear transformation is alteredover thecreation of free volume. In this way, we can conclude that the Argon's model clarifies the inhomogeneous deformation.

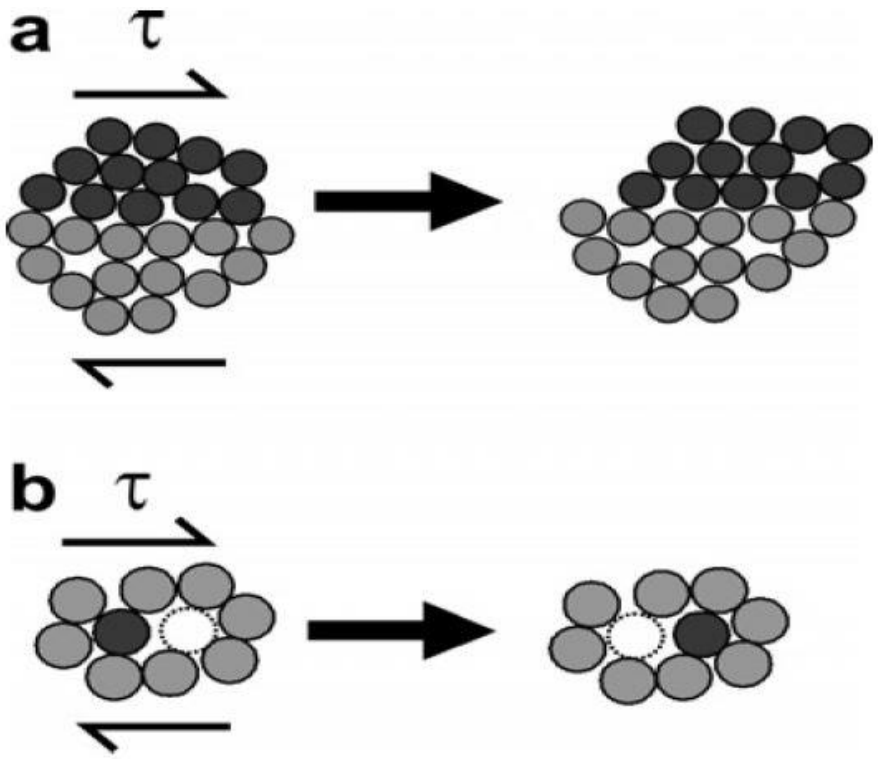


Fig. 2.5: shows deformation behaviour for amorphous metals, contains (a) a Shear Transformation Zone(STZ) [32] and (b) a local atomic jump[33].

## 2.3.1 Plastic deformation

There are different theories portraying the plastic deformation mechanism of metallic glasses.The strain-accomodationneighborhood improvement hypothesis was purposed by Argon. As per Argon, in plastic deformation strains are created because of neighborhood shear changes which are nucleated while stress are applied and allocation of thermal variations are about the free volume sites of the amorphous or glassy structure[32]. As per spaepen model, the deformation mechanism of metallic glasses are strongly depends upon stress and temperature.Fig.2.6 shows the deformation behaviour of metallic glasses in which strain rates lines (solid lines) are independent of temperature. Metallic glasses over the liquid temperature $T_{liq}$ acts like a Newtonian liquid. Viscosity increases as the cooling rate of the liquid increases. In

the temperature range between $T_x$ and $T_g$ deformation of metallic glasses strongly depends upon applied strain rate.

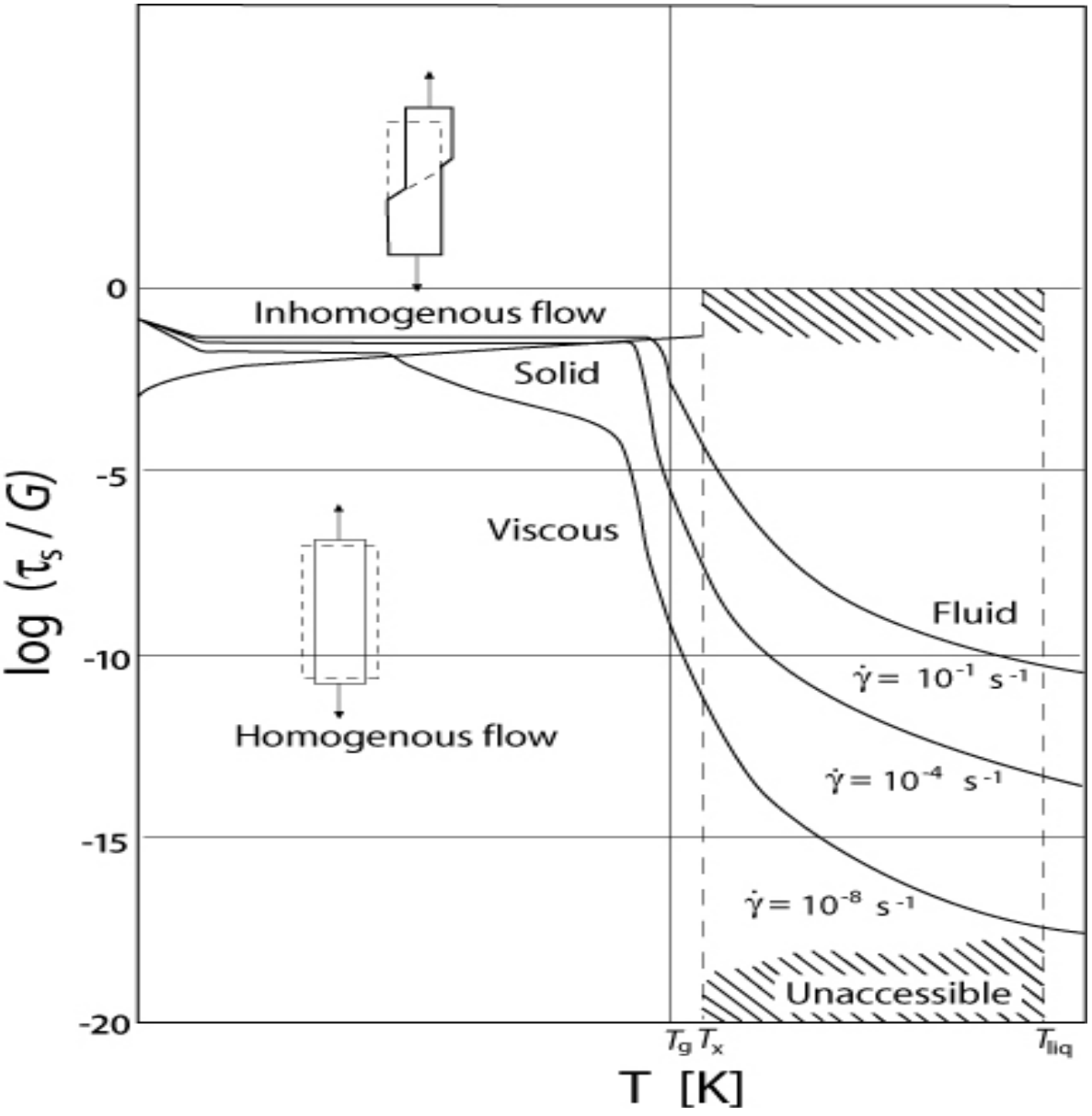


Fig.2.6: Deformation mechanism of metallic glasses[33]

Depending upon temperature, deformation of metallic glasses can be divide into two types: one is homogenous and another one is inhomogenous deformation. These are briefly described below:

### 2.3.2 Homogenous deformation

Normally homogenous deformation takes place near the glass transition temperature and it depends upon the strain rate. If the strain rate is low, it act like as Newtonian fluid and it behaves like Non-newtonianfliud when strain rate is high. Homogeneous deformation of metallic glasses is separated into three regions explicitly: deformation occurs below Tg, in between Tg and Tx (crystallization temperature) and beyondTx [35].

- When T <Tg: In the creep test studies (Mulder et al.) on $Fe_{40}Ni_{40}B_{20}$metallic glass at raised temperature 523 and 548 K which is beneath the glass move temperature (700 K) and applied stress(>1.0 GPa)it was inferred that activation energy is equivalent to eutectic crystallization underneath the glass transition temperature.

  Kawamura et al. [36]considered the deformation properties of glass $Zr_{65}Al_{10}Ni_{10}Cu_{15}$whose Tg and Tx are individually 652 K and 757 K. After the study they establish that the strain rate sensitivity of this amalgam is low (m < .25) and tensile elongation is likewise low (< 100%). From the above results we may infer that the deformation of metallic glasses close to the temperature Tg are described by a low strain rate sensitivity and flexibility.

- When T <Tx: Normally metallic glass alloys are solidified and generate nanocrystalline structure over the Tx. At temperature T material does not exist in amorphous shape but instead nanocrystalline. Analysts are not ready to get more data of deformation of metallic glasses over the temperature Tx. Kawamura et al. [36] clarify that the ductility of BMGs are for the most part substantial in the supercooledliquid region however definitely decreases over the Tx.

- WhenTg< T <Tx:This area is called supercooledliquid region. Khonik and Zelenskiy [37] had discovered some mechanical information after the investigation of 15 distinctive metallic glasses, they found that if the estimation of ΔT is expansive superplasticity happens in metallic glass composites, where Δ= Tx-Tg .if ΔT is bigger, tensile elongation is large. They also suggest that with increment in rate of heatingelongation is bigger. Ascloser rate of heating and bigger estimation of ΔT minimizes the crystallization amid superplastic deformation. Table 2.1 demonstrates the thermal and mechanical properties of metallic glasses.

Table 2.1: Deformation statistics of BMGs in super cooled region [35].

| Alloy (in at. %) | Tg(k) | Tx (k) | m value | Ductility |
|---|---|---|---|---|
| $La_{55}Al_{25}Ni_{20}$ | 480 | 520 | 1 | 1800 (T) |
| $Zr_{65}Al_{10}Ni_{10}Cu_{15}$ | 652 | 757 | 0.8-1 | 340 (T) |
| $Pd_{40}Ni_{40}P_{20}$ | 578-597 | 651 | 0.4-1 | 1260(T) |
| $Zr_{55}Cu_{30}Al_{10}Ni_{5}$ | 683 | 763 | 0.5-1 | Nil (c) |
| $Pd_{40}Ni_{40}P_{20}$ | 589 | 670 | 0.5-1 | 0.94 (c) |
| $Zr_{65}Al_{10}Ni_{10}Cu_{15}$ | 652 | 757 | 0.83 | 750 (T) |
| $Zr_{55}Al_{10}Cu_{30}Ni_{5}$ | 670 | 768 | 0.5-0.9 | 800 (T) |
| $Cu_{60}Zr_{20}Hf_{10}Ti_{10}$ | 721 | 766 | .3-.61 | 0.78 (C) |
| $Zr_{52.5}Al_{10}Cu_{22}Ti_{2.5}Ni_{13}$ | 659 | 761 | 0.5-1 | > 1.0 (C) |
| $Zr_{52.5}Al_{10}Ti_{5}Cu_{17.9}Ni_{14.6}$ | 358 | 456 | 0.45-0.55 | 650 (T) |
| $Zr_{41.25}Ti_{13.75}Ni_{10}Cu_{12.5}Be_{22.5}$ | 614 | 698 | 0.4-1 | 1624(T) |
| $Ti_{45}Zr_{24}Ni_{7}Cu_{8}Be_{16}$ | 601 | 648 | Nil | 1.0 (T) |
| $La_{60}Al_{20}Ni_{10}Co_{5}Cu_{5}$ | 451 | 523 | 1.0 | Nil |

### 2.3.3 Inhomogenous deformation

In general, the inhomogeneous deformations occurs due to non-uniform distribution of free volume, which comes from thermal fluctuation and quenching process. At low temperature i.e; below Tg deformation is inhomogeneous and is accepted by thin shear band, highly localized, restrictive macroscopic plasticity. Usually in tensile deformation, enlarge of shear band consequences low plastic deformation which leads to fracture of materials. During inhomogenous deformation, notched plastic flow is observed in different modes of loading like bending, compression and tearing. The most important reason of inhomogenous deformation are notched plastic flow and shear bands and also these two properties are strong function of strain rate [38].

## 2.4 Effect of Strain rates and Temperatures on MGs

Duhamel et al.[39] clarify that the glassy alloys under compressive behaviour, with increasing strain rates the yield strength and plastic strain increases significantly at room temperatures.

Hajloui et al.[40] explains that the amorphous alloy during tensile behaviour, with increasing strain rates the yield strength and elastic strain decreases significantly.

Ge et al.[41] explains that the model alloy, with increasing temperatures the plastic strain increases with decreasing yield strength. At higher strain rates, the alloy shows Non-newtonian behaviour and at lower strain rates, it shows Newtonian behaviour.

### 2.4.1 Effect of free volume on MGs

Launey et al.[42] explains with increasing cooling rate the free volume of the glassy alloy also increases. The deformation of MGs requires the existence of free volume. A reduction of free volume hinders the plastic deformation as a results the the alloy will undergo lower fracture toughness and longer fatigue lives. Latter alloy exhibit the fatigue crack initiation because of decrease in free volume.

## 2.5 Gaps in the literature

1. Several experimental and simulation deformation studies have been reported on the deformation mechanism and deformation behaviour of Cu-Zr metallic glasses [35-37]. However, there are seldom studies reported on the influence of cooling rate on the mechanical properties.
2. Stutural changes during deformation are seldom reported in literature.
3. Stress analysis during deformation is also not reported in literature.

# CHAPTER-3

# MODELING AND SIMULATION

# 3COMPUTATIONAL METHOD

## 3.1 Incentive

Computer simulation has been done in the trust of understanding the properties of get-together of atoms as far as their structure and the minute connections between them.This provides as a harmonize to traditional experiments, empowering us to learn something new, something that can't be discovered in different ways. The two principle families of simulation approaches are Molecular Dynamics (MD) and Monte Carlo (MC); also, here is an entire scope of crossover strategies which consolidate highlights from both. In this address we should focus on MD. The undeniable preference of MD over MC is that it gives a course to dynamical properties of the framework: transport coefficients, time-subordinate reactions to irritations, deformation properties and spectra.

## 3.2 Molecular Dynamics (MD)

Molecular Dynamics (MD) is a computer simulation method where the time development of a set of interacting atoms and molecules of a system subsequently integrating their equations of motion.The particles and atoms of the framework are permitted to communicate for a period of time giving a perspective of their movement.The directions of the interfacing particles are dictated by numerically settling Newton's comparisons of movement where strengths between the particles and potential vitality are characterized by atomic mechanics power fields. The Newton’s equation of motion can be articulated as:-

$$F_i = m_i a_i$$

$$a_i = \frac{d^2 r_i}{dt^2}$$

Where F= force between the interacting particles

$m_i$= mass of each particle
$a_i$ = Acceleration of each particle
$r_i$ = particle position

The following steps are followed while doing molecular dynamics simulation:-

- The depiction of introductory positions and velocity of each atom are done.
- The interatomic possibilities are utilized to examine the strengths between these molecules. After a little interim of time the powers are recognized, the nuclear positions and speeds changes to another state.
- The recurrence of recognizable proof of positions and velocity is completed until the end of the simulation.
- The energy remains constant due to no mass modification occurs in the system throughout the simulation.

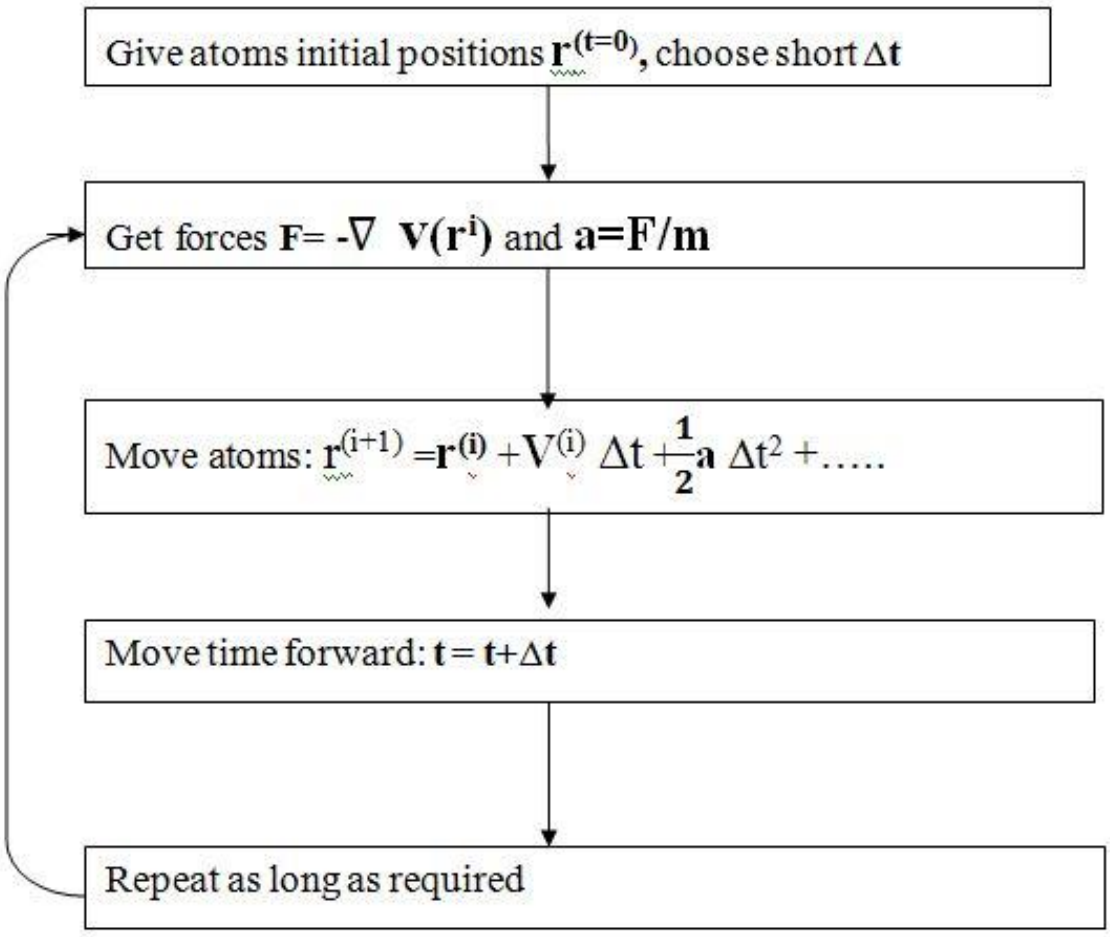


Fig.3.1: Simulation hierarchy flowchart

## 3.3 Boundary Condition

For successively MD simulation, the decision for the Boundary Condition (BC) is extremely essential. Because of the confinements in computer productivity; Molecular Dynamic recreation can give a little gathering of molecules of the framework under analysis. For the most part there are two most vital limit conditions, one is Isolated Boundary condition and another is Periodic Boundary Condition. In Isolated Boundary Condition the molecules or particles connect with themselves however can't associate with outside particles. At the same time, in the event of Periodic Boundary Condition the particles communicate with themselves as well as associate with outside particles.

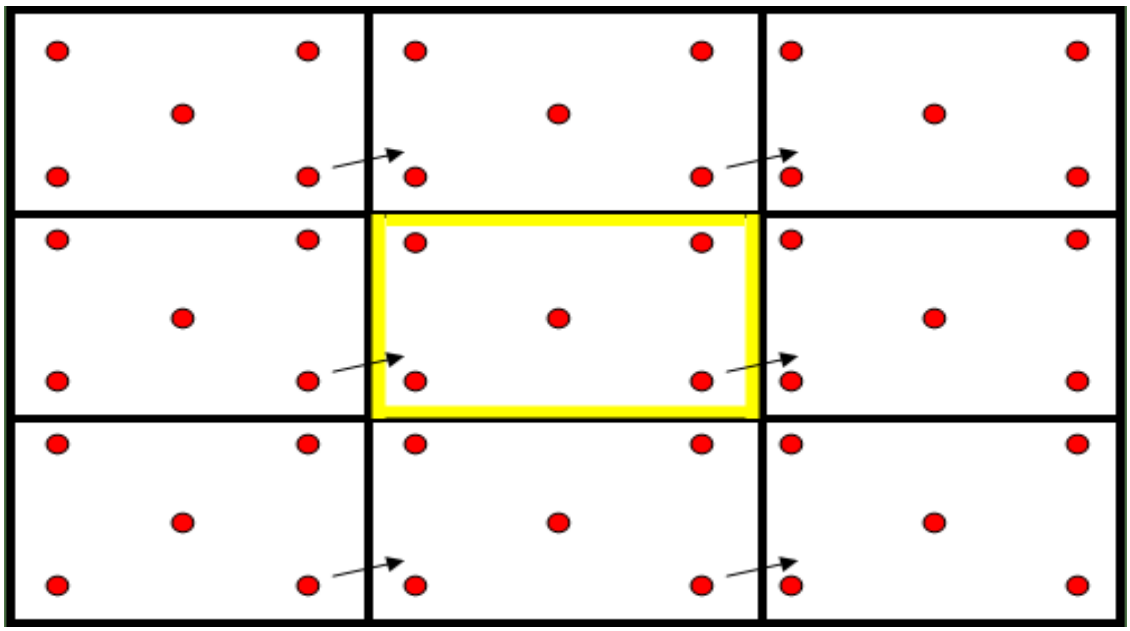

Fig. 3.2: 2-D representation of Boundary Conditions

## 3.4 Interatomic Potentials

Interatomic potential is characterized as the cooperation between pair of molecules or gathering of particles in a fluid stage.On the off chance that pairing happens between the atoms, potential must be having both the natures i.e. attractive and repulsive.It is the important part of MD simulation. In MD simulation we revise millions of particles and there are different type of computation is required like- transport calculation (diffusion, thermal conductivity, viscosity),

mechanical quantities (elastic constant, plastic yield), and also the modelling of compound phenomena (shear band localization). Output results bank on the eminence of interatomic potential. On the off chance that basic possibilities are utilized, there is less accurateness while for extensive simulation, more complex potential give a superior result. Such a large number of quantities of possibilities are utilized as a part of simulation procedure. There are some important potential are described underneath:

### 3.4.1 Empirical Potential

It is the mix of intra-atomic and between sub-atomic commitments. An intra-atomic potential vitality capacity contains the short-range or reinforced bit of the potential while between sub-atomic potential vitality capacities contains the long range or non-fortified connections. Numerical manifestation of observational potential is given beneath:

$$V = V_{\text{short-range}} + V_{\text{long-range}}$$

### 3.4.2 Pair Wise Potentials

In Molecular Dynamics, various type of pair potential available to depict numerous atom/molecule interactions, for instance Born-Lande potential, which is frequently used to define ion lattice.The Morse potential is an experimental potential that clarifies the extending of a substance bond with its unbalanced design which will be discovered to be troublesome to pack a bond as contrasted with pulling a bond separated. Also in pair wise potentials, the total energy is calculated from the sum of energy contributions between pairs of atoms.

### 3.4.3 Multiple-body Potentials

In multiple-body potentials, the potential energy incorporates the impacts of three or more particles associating with every other. In pair-wise potentials, worldwide interfaces in the system also occur, but they happen only through pairwise terms. But in multiple-body potentials, the potential energy can't be found by a whole over sets of atoms, as these communications will be ascertained unequivocally as a mix of higher-order terms.

### 3.4.4 Embedded Atom Method

EAM method plays a vital role in molecular dynamics simulation. In EAM, total energy is the addition of separation between the atoms & its neighbour atoms.The EAM method will be figured sober-mindedby fitting to the sublimation energy, balance cross section consistent, elastic constants and vacancy creation energies of the pure metals and the heats of the solutions of the binary alloys. If there are N numbers of atoms in the system, then the total energy of the system can be expressed as below:-

$$E_{total} = \sum_i F_i(\rho_{h,i}) + \frac{1}{2}\sum_{\substack{i,j \\ i \neq j}} \emptyset_{ij}(R_{ij})$$

## 3.5 Ensembles

Time midpoints are journalist to the outfit midpoints will be the major thought for assessing the simulation results. Mostly, MD simulation is carried out under some vital equilibrium ensembles. Some commonly used ensembles are itemized below:-

**Micro-canonical or NVE ensemble:**

The expansion of NVE is N (no. of atoms/molecules), V (volume) and E (energy). It is considered as total energy remains constant throughout the simulation.

**Canonical or NVT ensemble:**

In NVT, number of particles(N), Volume (V) and Temperature (T) are conserved. Here temperature is constant throughout the simulation for which it is also called as constant temperature molecular dynamics. In NVT, because of thermostat the endothermic & exothermic processes can be exchanged.

**Isothermal-Isobaric or NPT ensemble:**

In NPT, number of particles (N), Pressure (P) and Temperature (T) are conserved throughout the simulation.

**Isoenthalpic-Isobaric or NPH ensemble:**

In NPH, number of particles (N), Pressure (P) and Enthalpy (H) remains constant throughout the simulation.

## 3.6 Integration

In MD simulation, the forces should be incorporated for the movement of atoms. Because of million numbers of atoms participate in the simulation it is very tiresome and difficult to analyse a system. Therefore, a system is functional to a numerical integration method. Hence numerical integration method consists of several methods such as-Verlet algorithm, Velocity-Verlet algorithm, Leap-frog algorithm and Beeman's algorithm. Among them Verlet algorithm is essentially used in molecular dynamics simulation.

**Verlet Algorithm:**

In molecular dynamics, the most frequently used time integration algorithm is undoubtedly called Verlet algorithm.The fundamental thought is to compose two third-arrange Taylor extensions for positions***r(t),*** one frontward and one retrograde in time. The third order extents will be velocities ***v(t)***, acceleration ***a(t)*** and the third order derivative of positions ***b(t).***

$$r(t-\Delta t) = r(t) - v(t)\Delta t + \frac{1}{2}a(t)\Delta t^2 - \frac{1}{6}b(t)\Delta t^3 + O(\Delta t^4)$$

$$r(t+\Delta t) = r(t) + v(t)\Delta t + \frac{1}{2}a(t)\Delta t^2 + \frac{1}{6}b(t)\Delta t^3 + O(\Delta t^4)$$

By adding above expressions following expression can be derived:

$$r(t+\Delta t) = 2r(t) - r(t-\Delta t) + a(t)\Delta t^2 + O(\Delta t^4)$$

This is the basic form of Verlet Algorithm.

## 3.7 Application of Molecular Dynamics simulation

- ✓ Used to study the impact of neutrons and particle light on strong surfaces.
- ✓ It has wide applications in materials segments too where tests in regards to any issue are extremely hard to do in research centre conditions.
- ✓ It is basically utilized for simulation of bio-sub-atomic frameworks like protein synthesis and classification.

- ✓ It is additionally used to study different properties of metals, non-metals and compounds like high temperature behaviour, fatigue properties, deformation behaviour and tensile properties.

## 3.8 LAMMPS

LAMMPS (Large-Scale Atomic Molecular Massively Parallel Simulator) is a Molecular Dynamics program from Sandia National Laboratories. This is the basic code to do material simulation. LAMMPS can be utilized to model molecules or as a parallel molecule test system at the nuclear, meso, or continuum scale. It is utilized to run in single processor or run in parallel using message-passing parallelism (MPI).

The structure of a data script in LAMMPS is the particular case that takes after:

1. Initialization.
2. Atom and Lattice description.
3. Force fields.
4. Settings.
5. Run a simulation.

**The following commands describe the input file of the program:**

**Initialization:**

Definition of the units that will be utilized amid the simulationi.e. metal units are: distance ( Å), time( picoseconds), energy( eV), velocity( Å/ps), temperature(K), pressure(bar).

Units metal

Echo both

The boundary conditions that are used in LAMMPS are:

P P P

S P S

P F P

Where, “P” stands for periodic, “F” stands for non-periodic & fixed and “S” stands for non-periodic &shrink-wrapped.

Box dimensions are used in LAMMPS:

Dimension 3D or 2D.

**Atom & Lattice description:**

Atom_style atomic

region box block 0 50 0 100 0 50 units box

create_box 1 box

lattice fcc 3.61

**Force field:**

set region cu type/fraction 2 0.5 12393

Choice of interatomic potentials plays a vital role throughout the simulation:

pair_style eam/fs

pair_coeff * * CuZr_mm.eam.fs Cu Zr

**Setting:**

Energy minimization performs a important role in LAMMPS. Higher the energy

minimizationincreases the stabilization among the atoms and vice-versa.

```
minimize            1.0e-9 1.0e-6 1000 10000
thermo              100
thermo_style        custom step temp vol press potential energy kinetic energy total energy
```

The output of the LAMMPS simulation is printed into text files called dump file.It contains the information of the atom coordinates along with the velocities dumped at the required timestep.

```
dump                1 all atom 10000 q_bar_1013ks-1.lammpstrj
dump_modify         1 scale no
velocity            all create 300.0 873847 rot yes mom yes dist gaussian
```

**Run the simulation:**

```
fix                 1 all npt temp 300 1150 0.1 iso 0.0 0.00.2
run                 10000
unfix               1
fix                 1 all npt temp 1150 1150 0.1 iso 0.00.0 0.2
run                 50000
unfix               1
fix                 1 all npt temp 1150 270 0.1 iso 0.00.0 0.2
run                 10000
unfix               1
```

# CHAPTER-4

# RESULTS

# AND

# DISCUSSION

# 4.SIMULATION RESULTS

## 4.1 Creation of amorphous alloy

### 4.1.1 Creation of $Cu_{50}$-$Zr_{50}$ glassy alloy

There are three steps for the development of $Cu_{50}$-$Zr_{50}$ amorphous alloy. In the first step, heating the crystalline material from room temperature (300K) to 1150K, then holding for 100ps and then rapid cooling/quenching the model alloy to the room temperature.

In order to construct a glassy model a code is written and executed in LAMMPS. The following 'in. file' consists of set of commands that will construct a glassy model-

- This program is for obtaining quenched structure by melting $Cu_{50}$-$Zr_{50}$ alloy for 3d system.

```
Units           metal
Echo            both
atom_style      atomic
dimension       3
boundary        p p p
region          box block 0 50 0 100 0 50  units box
create_box      2 box

lattice         fcc 3.61
region          cu block 0 50 0 100  0 50 units box
create_atoms    1 region cu units box

# creating composition using set command for cu50zr50 alloy
Set             region cu type/fraction 2 0.5 12393

group           cu type 1
group           zr type 2

timestep        0.002
```

```
pair_style              eam/fs
pair_coeff              * * CuZr_mm.eam.fs Cu Zr

# Energy Minimization
 minimize               1.0e-3 1.0e-6 1000 10000

compute                 1 cu  msd
compute                 2 zr msd

thermo                  100
thermo_style            custom step temp  vol press pe ke etotal

dump                    1 all atom 10000 q_bar_1013ks-1.lammpstrj
dump_modify             1 scale no
log log5050_q_bar_10^13ks-1.data

velocity                all create 300.0 873847 rot yes mom yes dist gaussian

#fixes
compute                 myRDF all rdf 100
fix                 2   all  ave/time  1000  1  1000   c_myRDF  file  Cu_Zr_quench_large_restart.rdf
mode vector

fix                     1 all npt temp 300 1150 0.1 iso 0.0 0.0 0.2

run                     10000
unfix                   1

fix                     1 all npt temp 1150 1150 0.1 iso 0.0 0.0 0.2

run                     50000
unfix                   1
```

| | |
|---|---|
| fix | 1 all npt temp 1150 270 0.1 iso 0.0 0.0 0.2 |
| run | 10000 |
| unfix | 1 |

### 4.1.2 Radial Distribution Function (RDF) plots

Fig. 4.1(a) demonstrates the RDF plots of the $Cu_{50}$-$Zr_{50}$ crystalline model whichunmistakablyshows the sharp peaks for the crystalline nature while Fig. 4.1(b) shows the broad peak for quenched structure.

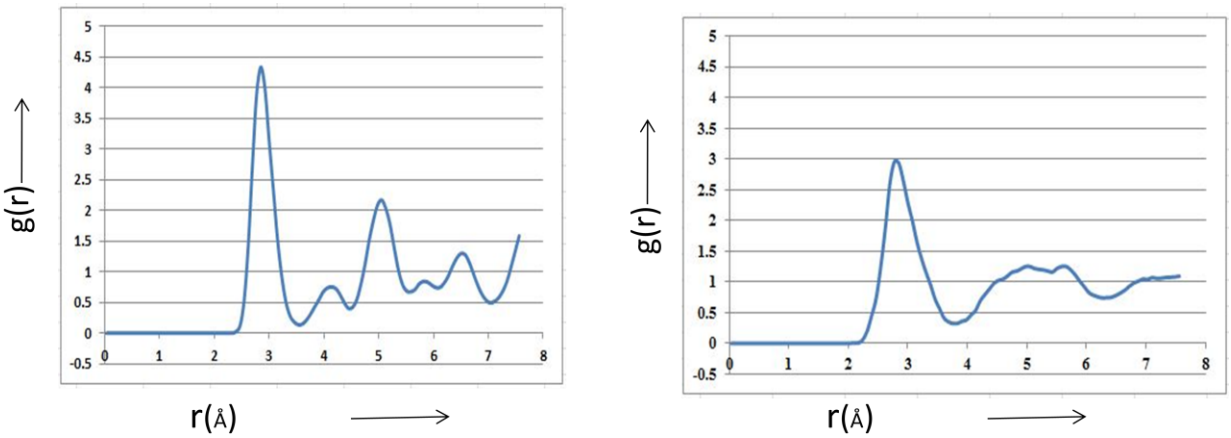


(a) (b)

Fig. 4.1: RDF plots for $Cu_{50}$-$Zr_{50}$ (a) crystalline structure (b) quenched structure.

### 4.1.3 Atomic position snapshots

With the help of Ovito snap shots we can clearly distinguish between crystalline structure and glassy structure. In Fig.4.2 (a), for crystalline structure we can observe all the atoms/molecules are arranged in perfect manner while in Fig.4.2 (b), for quenched structure all the atoms are arranged in random positions.

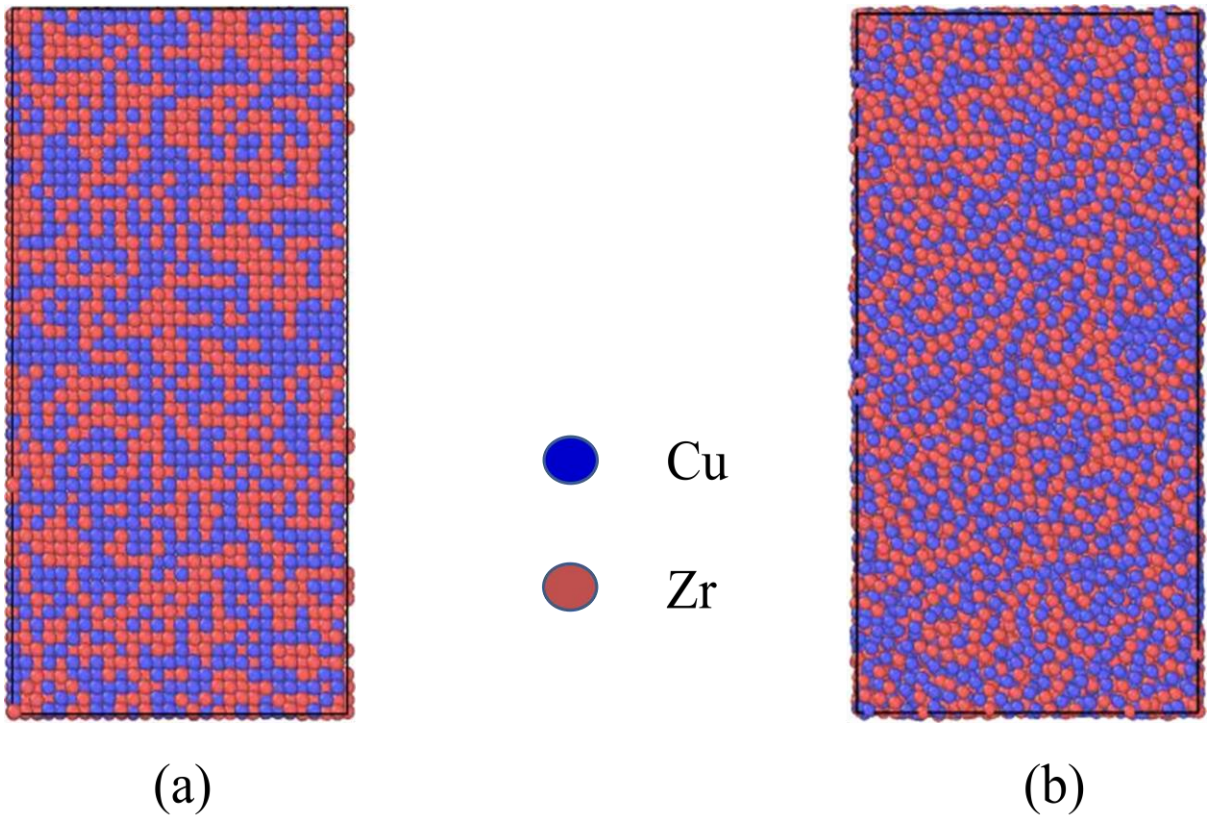


Fig. 4.2: Atomic position snap shots for $Cu_{50}$-$Zr_{50}$ (a) crystalline structure (b) quenched structure.

### 4.1.4 Volume-Temperature plot

Fig. 4.3(a) demonstrates during heating from 300K to 1150K, volume increases with increase in temperature. While Fig.4.3(b) shows after quenching at cooling rate $10^{13}$K/s, volume decreases with decrease in temperature.

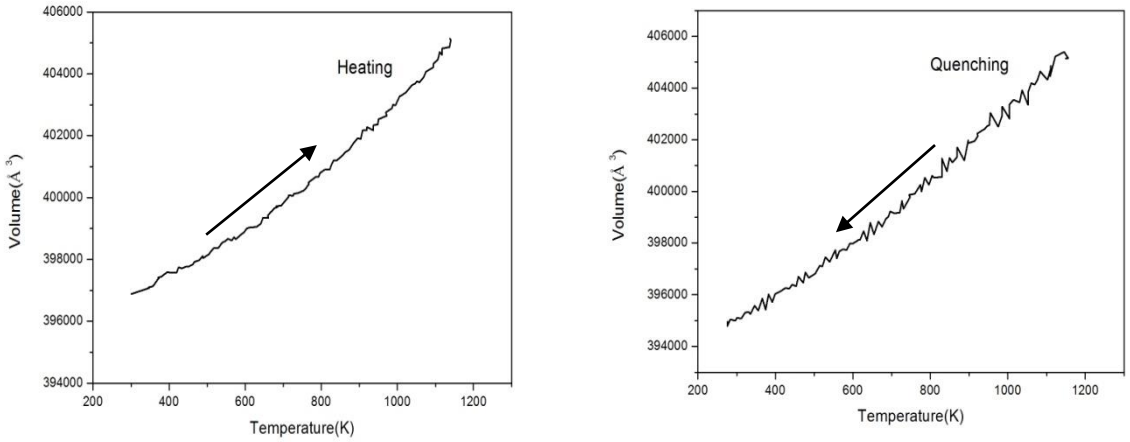


(a) (b)

Fig.4.3: Volume-Temperature plot during (a) heating and (b) quenching.

### 4.1.5 Change in Free-Volume in Volume-Temperature plot

Fig.4.4, represents with increasing cooling rate in the range of $10^{10}$K/s-$10^{14}$K/s, free volume increases correspondingly. With higher free volume material will extend effortlessly under low stress.

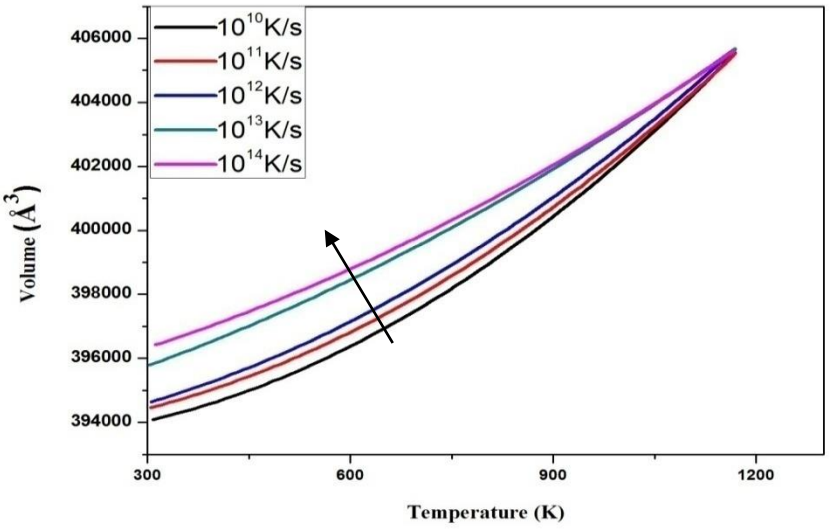


Fig.4.4: Volume Vs Temperature plot at different cooling rate.

### 4.2 Tensile deformation of quenched specimen

After the development of glassy model alloy, uniaxial tensile deformation has been done at distinctive temperatures viz. 300K, 200K, 100K, 50K and 10K and strain rates viz. $1\times10^{9}s^{-1}$, $1\times10^{10}s^{-1}$, $1\times10^{11}s^{-1}$ and $1\times10^{12}s^{-1}$, in order to study the effect of free volume, temperatures and strain rates on the model alloy. After tensile test, mechanical properties such as ultimate tensile strength and yield strength has been evaluated.

- This program is for obtaining tensile behavior of $Cu_{50}$-$Zr_{50}$ for 3D system ($10^{9}$ $s^{-1}$ strain rate).

```
units           metal
echo            both
atom_style      atomic
dimension       3
boundary        s p s
read_data       CuZr_cooling_10_13.txt
timestep        0.002
pair_style      eam/fs
pair_coeff      * * CuZr_mm.eam.fs Cu Zr
# Energy Minimization
 minimize       1.0e-9 1.0e-6 1000 1000
compute         1 all  stress/atom
compute         csym all centro/atom fcc
compute         peratom all pe/atom
variable        tmp equal ly
variable        lo equal ${tmp}
variable        strain equal (ly-v_lo)/v_lo
```

```
variable                p1 equal "-pxx/10000"

variable                p2 equal "-pyy/10000"

variable                p3 equal "-pzz/10000"

variable                p12 equal "-pxy/10000"

variable                p23 equal "-pyz/10000"

variable                p13 equal "-pxz/10000"


variable                fm equal "(v_p2+v_p3+v_p1)/3" ##### Hydrostatic stress

variable                fv equal "sqrt(((v_p2-v_p3)^2+(v_p3-v_p1)^2+(v_p1-
        v_p2)^2+6*(v_p12^2+v_p23^2+v_p13^2))/2)" ######Von Mises Stress

variable                t equal "v_fm/v_fv"

variable                fd equal (((v_p2-v_fm)*(v_p3-v_fm)*(v_p1-v_fm))-(v_p12)^2*(v_p3-
v_fm)-(v_p13)^2*(v_p2-v_fm)-(v_p23)^2*(v_p1v_fm)+2*v_p12*v_p23*v_p13)####Deviatoric
Von Mises stress

# principal stresses

variable                I1 equal "(v_p1+v_p2+v_p3)"

variable                I2 equal "((v_p1)*(v_p2))+((v_p2)*(v_p3))+((v_p1)*(v_p3))-(v_p12)^2-
(v_p23)^2-(v_p13)^2"

variable                I3 equal "((v_p1)*(v_p2)*(v_p3))-((v_p1)*((v_p23)^2))-
((v_p2)*((v_p13)^2))-((v_p3)*((v_p12)^2))+2*(v_p12)*(v_p23)*(v_p13)"

variable                A equal "(acos(((2*(v_I1)^3)-9*(v_I1)*(v_I2)+27*(v_I3))/(2*((v_I1)^2-
(3*(v_I2)))^(3/2))))/3"

variable                s1 equal "((v_I1)/3)+(2/3)*(sqrt((v_I1)^2-(3*(v_I2))))*cos(v_A)"

variable                s2 equal "((v_I1)/3)+(2/3)*(sqrt((v_I1)^2-
(3*(v_I2))))*cos((v_A)+(2*PI)/3)"

variable                s3 equal "((v_I1)/3)+(2/3)*(sqrt((v_I1)^2-
(3*(v_I2))))*cos((v_A)+(4*PI)/3)"
```

```
thermo                  10000

thermo_style            custom step temp  vol press pe ke etotal

dump                    1 all custom 10000 tension_CuZr.lammpstrj id type x  y z

dump                    2 all cfg 10000 dump.tensile_CuZr*.cfg mass type xs ys zs c_csym
c_peratom

dump                    3 all custom 10000 stress_peratom* id type x y z c_1[1] c_1[2] c_1[3]
c_1[4] c_1[5] c_1[6]


log                     NVTlog5050_tensile_CuZr.data

velocity                all create 300 8173847 rot yes mom yes dist gaussian

#temperature controller

fix                     1 all nvt temp 300 300 0.1

# tensile deformation

 fix                    2 all deform 1  y erate 0.001 units box

fix                     3 all print 10000 "${strain} ${p2}" file stress_strain_data.txt

fix                     def all print 1 "${strain} ${p2} ${s1} ${s2} ${s3} ${fm} ${fv} ${t}
${fd}" file CuZr_tension_von.txt

run                     1000000
```

### 4.2.1 Effect of strain rates

Fig.4.5,demonstratethe tensile deformation of various Stress Vs Strain plots of $Cu_{50}$-$Zr_{50}$ model alloy at different strain rates in the range of $10^{9}$ $s^{-1}$ -$10^{12}$ $s^{-1}$and temperatures viz. 300K, 200K, 100K, 50K and 10K. From the figure, it has been shown that with increasing strain rates and decreasing temperatures, the stress value also increases significantly.

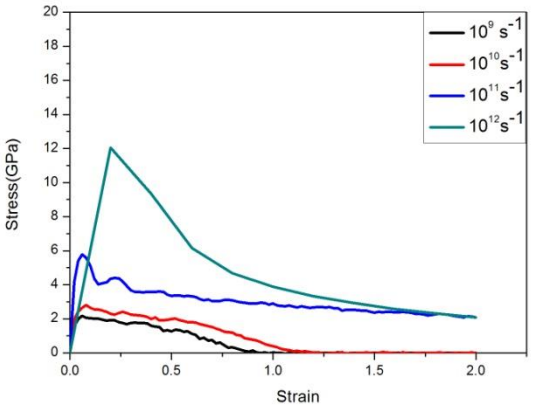


(a)

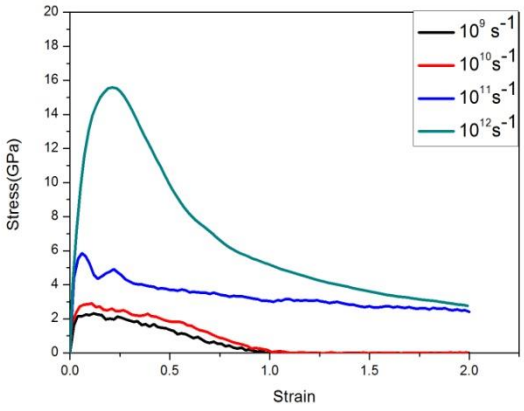


(b)

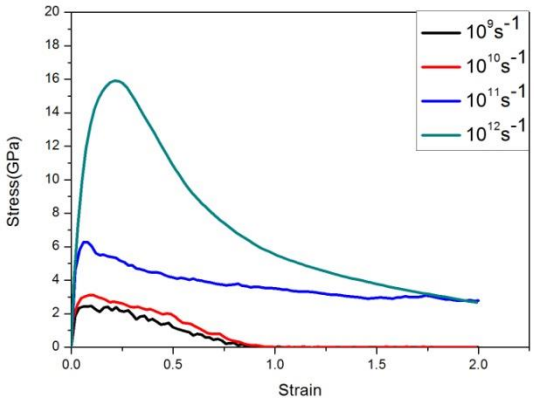


(b)

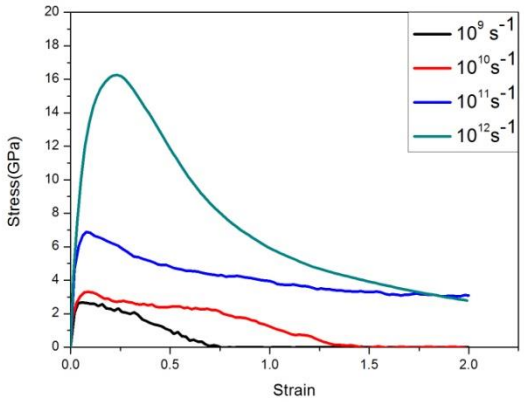


(d)

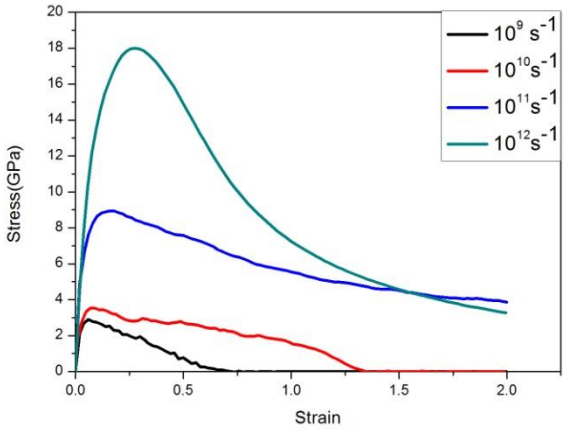


(e)

Fig.4.5: Shows variation ofsrtain rates in the range of $10^{9}$ $s^{-1}$– $10^{12}$ $s^{-1}$ of model alloy at different temperatures (a) 300K (b) 200K (c) 100K (d) 50K (e) 10K.

### 4.2.2 Atomic positionsnap shots

Ovito software is used to imagine the actions carried out in MD simulation. With the help of this software we can observe how the atoms are affecting in Fig.4.6, in different strain conditions viz. 0%, 50%, 80% and 100% at $10^9$ $s^{-1}$ strain rate. From the below figure, we can detect that at 0% strain value, model alloy is in glassy form, successively with increasing in strain value, the model alloy is deforming and at 50% and 80% necking can be witnessed and finally at 100% strain value, the model alloy has been deformed.

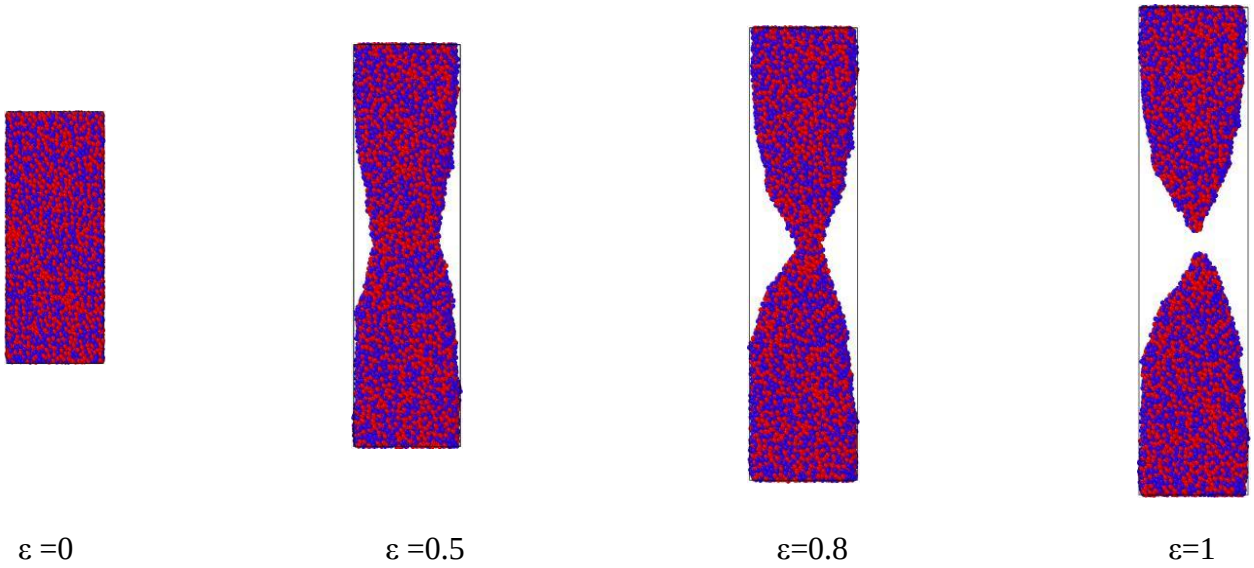

ε =0 ε =0.5 ε=0.8 ε=1

Fig.4.6: Snapshots showing atomic arrangement of tensile deformation at different strain values for T=300 K andat strain rate=$10^9 s^{-1}$.

#### 4.2.2.1 Yield strength variation

The simulation results focused on the effect of yield strength on$Cu_{50}$-$Zr_{50}$ model alloy at different strain rates, which are arranged in Table 4.1. From Table 4.1,it has been shown that theYield Strengthsignificantlyvaries w.r.t different strain rates. The value of yield strength at$10^9$ $s^{-1}$strain rate at room temperature is found to be 1.59 GPa but in higher strain rate($10^{12}$ $s^{-1}$) yield strength value is achieved 4.54 GPa and simultaneously with varying temperatures, the yieldstrength value also varies. The effect of different strain rate on yield strength of $Cu_{50}$-$Zr_{50}$alloy is depicted in Fig.4.7 .

Table 4.1: Yield strength variation w.r.t different strain rates of $Cu_{50}$-$Zr_{50}$ model alloy.

| Model Alloy | Strain Rate ($ps^{-1}$) | Yield Stregth(GPa) (300K) | Yield Stregth(GPa) (200K) | Yield Stregth(GPa) (100K) | Yield Stregth(GPa) (50K) | Yield Stregth(GPa) (10K) |
|---|---|---|---|---|---|---|
| $Cu_{50}$-$Zr_{50}$ | 0.001 | 1.59 | 1.68 | 1.93 | 2.11 | 2.19 |
| | 0.01 | 1.69 | 1.78 | 1.83 | 1.86 | 1.92 |
| | 0.1 | 4.34 | 4.45 | 4.73 | 4.89 | 5.16 |
| | 1 | 4.54 | 4.60 | 4.67 | 4.77 | 5.24 |

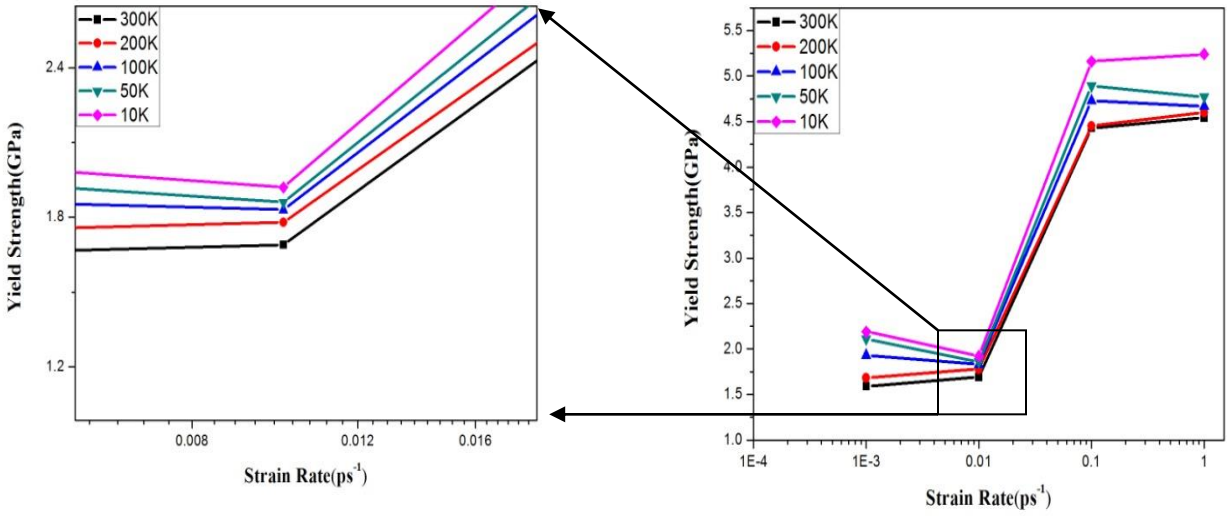


Fig.4.7: Yield strength vs strain rate plot.

### 4.2.2.2 Ultimate tensile strength variation

The simulation results focused on effect of UTS on $Cu_{50}$-$Zr_{50}$ model alloy at different strain rates, which are arranged in Table 4.2. From Table 4.2,it has been shown that the UTS significantlyvaries w.r.t different strain rates. The value of UTS at$10^9$ $s^{-1}$strain rate at room temperature is found to be 2.16 GPa but in higher strain rate ($10^{12}$ $s^{-1}$ ) UTS value is achieved 12 GPa and simultaneously with varying temperatures, the UTS value also varies. The effect of different strain rate on yield strength of $Cu_{50}$-$Zr_{50}$alloy is depicted in Fig.4.8.

Table 4.2: Ultimate tensile strength variation w.r.t different strain rates of $Cu_{50}$-$Zr_{50}$ model alloy.

| Model Alloy | Strain Rate ($ps^{-1}$) | UTS (GPa) (300K) | UTS (GPa) (200K) | UTS (GPa) (100K) | UTS (GPa) (50K) | UTS (GPa) (10K) |
|---|---|---|---|---|---|---|
| $Cu_{50}$-$Zr_{50}$ | 0.001 | 2.16 | 2.31 | 2.45 | 2.66 | 2.90 |
| | 0.01 | 2.78 | 2.89 | 3.11 | 3.29 | 3.52 |
| | 0.1 | 5.78 | 5.84 | 6.25 | 6.88 | 8.94 |
| | 1 | 12 | 15.57 | 15.90 | 16.24 | 17.98 |

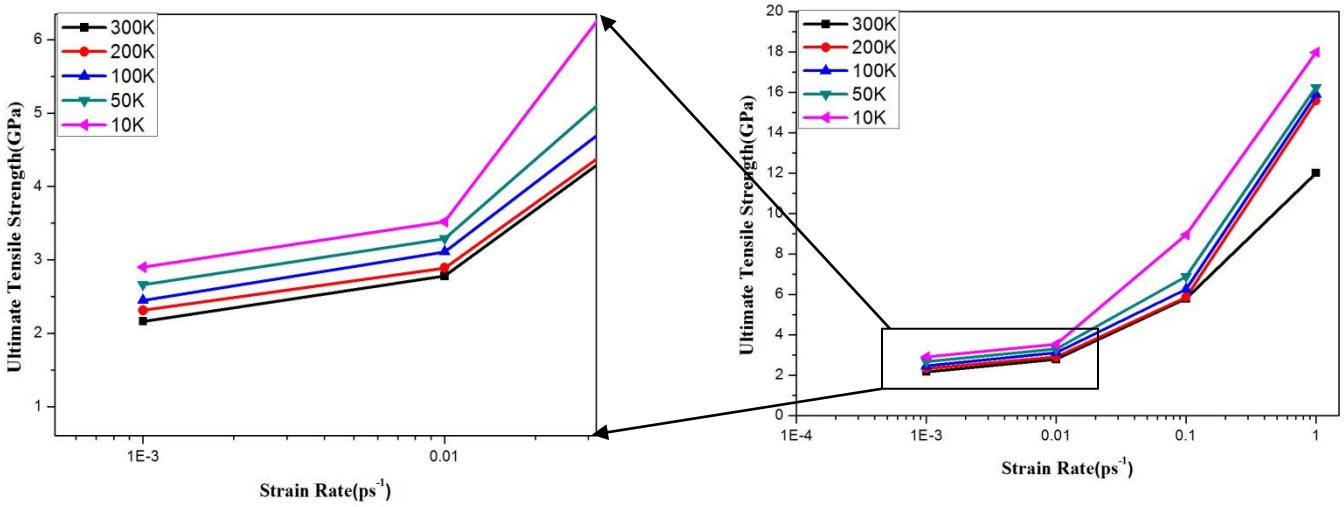


Fig.4.8: Ultimate tensile strength vs strain rate plot.

### 4.2.3 Effect of Temperatures

Fig.4.5showsthe tensile deformation of stress vs strain plots of $Cu_{50}$-$Zr_{50}$model alloy at different temperatures at viz. 300K, 200K, 100K, 50K, 10K at two different strain rates ($10^9$ $s^{-1}$ and $10^{12}$ $s^{-1}$) . It has been revealed that with decreasing temperatures the value of stress increases significantly.

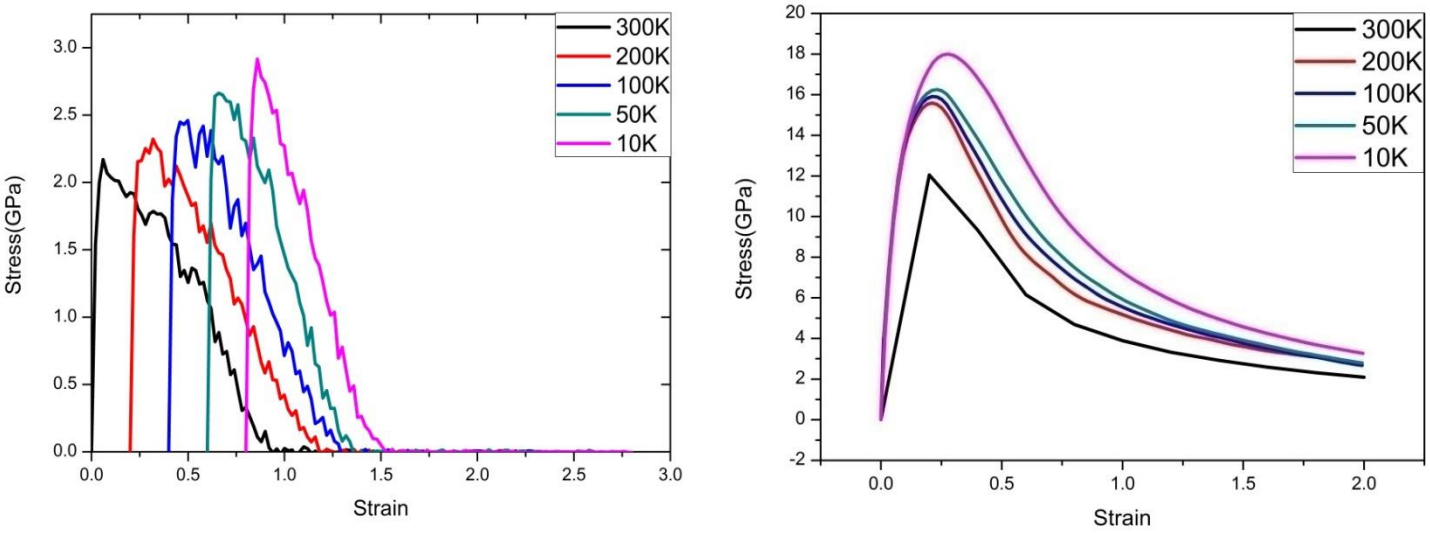


Fig.4.9: Shows variation oftemperatures(300K, 200K, 100K, 50K and 10K) of model alloy at two different strain rates (a) $10^{9}$ $s^{-1}$ (b) $10^{12}$ $s^{-1}$.

#### 4.2.3.1 Yield strength variation

The simulation results focused on effect of yield strength on $Cu_{50}$-$Zr_{50}$ model alloy at different temperatures, which are arranged in Table 4.3 . From Table 4.3, it has been shownthat theYield Strength significantlyvaries w.r.t different temperatures. At room temperaturethe value of yield strength is found to be 1.59 GPa but in lower temperature(10K) yield strength value is found to be2.19 GPa and simultaneously with varying strain rates, the yield strength value also varies. The effect of different temperatures on yield strength of $Cu_{50}$-$Zr_{50}$alloy is depicted in Fig.4.10.

Table 4.3: Yield strength variation w.r.t different temperatures of Cu50-Zr50 model alloy

| Model Alloy | Temperatures (K) | Yield Strength(GPa) (0.001 $ps^{-1}$) | Yield Strength(GPa) (0.01 $ps^{-1}$) | Yield Strength(GPa) (0.1 $ps^{-1}$) | Yield Strength(GPa) (1 $ps^{-1}$) |
|---|---|---|---|---|---|
| | 300 | 1.59 | 1.69 | 4.34 | 4.54 |

| | | | | | |
|---|---|---|---|---|---|
| $Cu_{50}$-$Zr_{50}$ | 200 | 1.68 | 1.78 | 4.45 | 4.60 |
| | 100 | 1.93 | 1.83 | 4.73 | 4.67 |
| | 50 | 2.11 | 1.86 | 4.89 | 4.77 |
| | 10 | 2.19 | 1.92 | 5.16 | 5.24 |

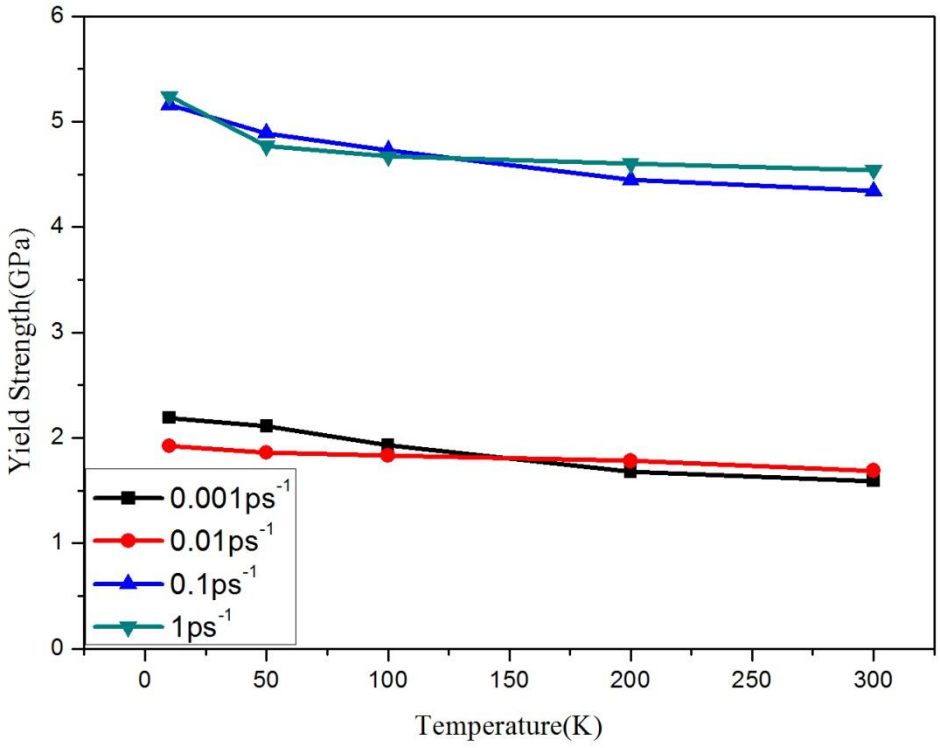


Fig.4.10: Yield strength vs Temperature plots.

#### 4.2.3.2 Ultimate Tensile Strength variation

The simulation results focused on effect of UTS on $Cu_{50}$-$Zr_{50}$ model alloy at different temperatures, which are arranged in Table 4.4. From Table 4.4,it has been shown that the UTS significantlyvaries w.r.t different temperatures. At room temperature the value of UTS is found to be 2.16 GPaand in lower temperature (10K) UTS value is found to be2.90 GPa and simultaneously with varying strain rates, the UTS value also varies. The effect of different temperatures on ultimate tensile strength of $Cu_{50}$-$Zr_{50}$alloy is depicted in Fig.4.11.

Table.4.4:Ultimate tensile strength variation w.r.t different temperatures of $Cu_{50}$-$Zr_{50}$ model alloy.

| Model Alloy | Temperatures (K) | Ultimate Tensile Strength (GPa) ($0.001\ ps^{-1}$) | Ultimate Tensile Strength (GPa) ($0.01\ ps^{-1}$) | Ultimate Tensile Strength (GPa) ($0.1\ ps^{-1}$) | Ultimate Tensile Strength (GPa) ($1\ ps^{-1}$) |
|---|---|---|---|---|---|
| $Cu_{50}$-$Zr_{50}$ | 300 | 2.16 | 2.78 | 5.78 | 12 |
| | 200 | 2.31 | 2.89 | 5.84 | 15.57 |
| | 100 | 2.45 | 3.11 | 6.25 | 15.90 |
| | 50 | 2.66 | 3.29 | 6.88 | 16.24 |
| | 10 | 2.90 | 3.52 | 8.94 | 17.98 |

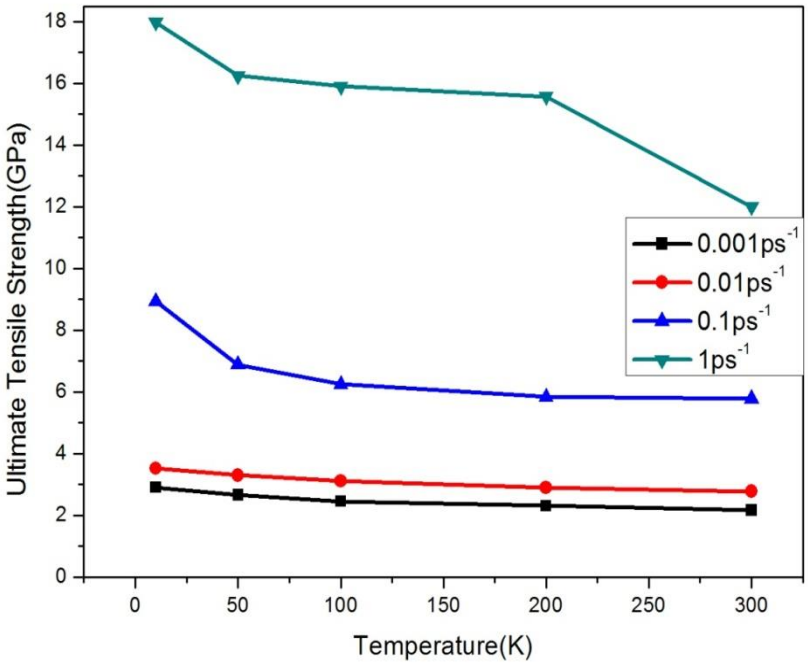


Fig.4.11: Ultimate tensile strength vs Temperature plots.

### 4.2.4 Effect of free volume

From Fig.4.12, atdifferent strain rates of $Cu_{50}$-$Zr_{50}$ model alloy, the ultimate tensile strength decreaseswith increasing cooling rate from $10^{11}$K/s-$10^{14}$K/s. With higher free volume material will extend effortlessly under low stress. From Table 4.5, it has been shown that the excess free volume significantly varies w.r.t different cooling rate. At cooling rate $10^{12}$ K/s the value of excess free volume is found to be 98.33 Å and at higher cooling rate ($10^{14}$ K/s) the value is found to be 1815.04 Å. At the same time increasing cooling rates, the value of change in yield strength and ultimate tensile strength decreases.

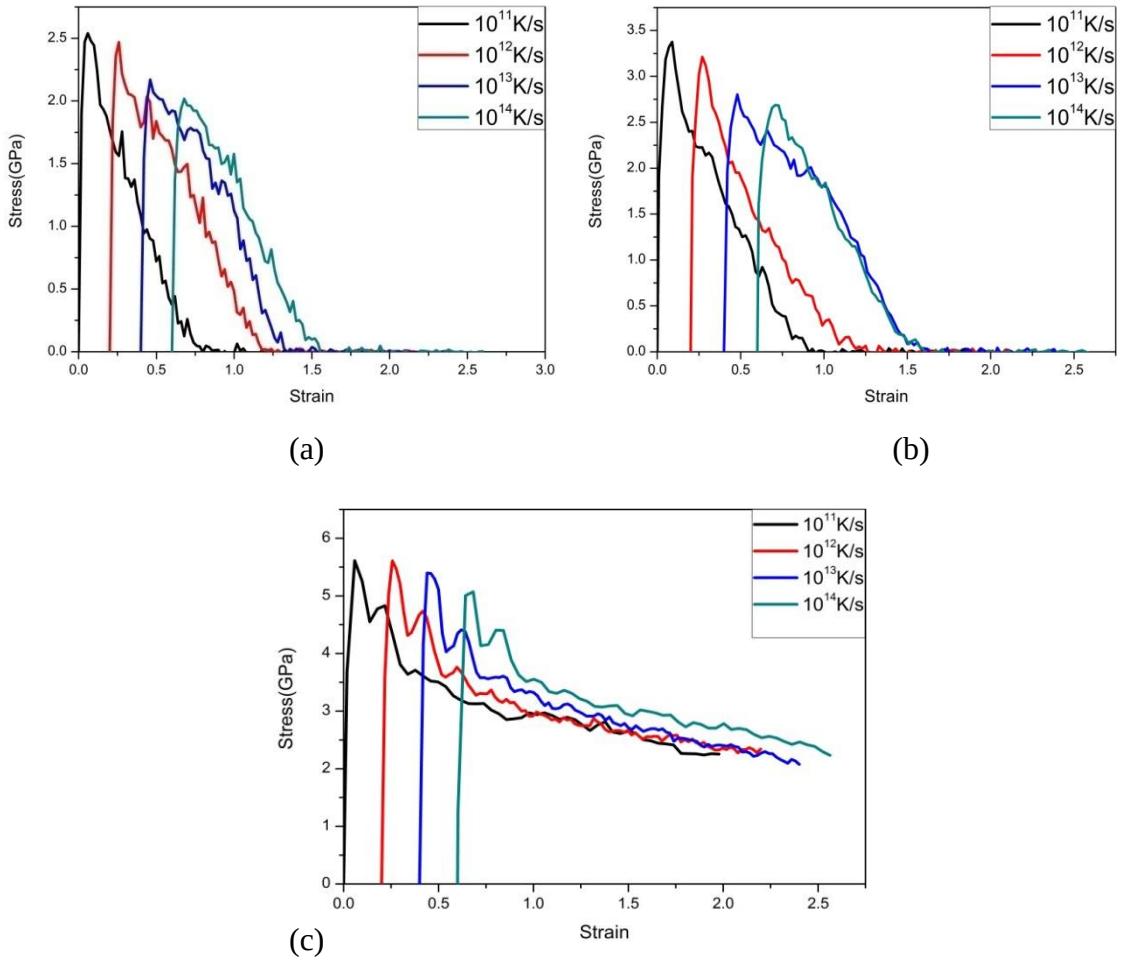


(c)

Fig.4.12: Stress Vs. Strain plots of different cooling rates at different strain rates (a) $10^{9}$ $s^{-1}$ (b) $10^{10}$ $s^{-1}$ (c) $10^{11}$ $s^{-1}$.

Table 4.5: Yield strength and Ultimate tensile strength variation w.r.t different cooling rate of $Cu_{50}$-$Zr_{50}$ model alloy.

| Cooling rate(K/s) | Volume (Å) | Excess free volume | Fraction of free volume | Yield strength (GPa) | UTS (GPa) | Change in Y.S | Fraction of Y.S | Change in UTS | Fraction of UTS |
|---|---|---|---|---|---|---|---|---|---|
| $10^{11}$ | 394507.06 | - | - | 1.96 | 2.54 | - | - | - | - |
| $10^{12}$ | 394506.79 | 98.33 | 0.0002 | 1.92 | 2.46 | 0.04 | 0.02 | 0.08 | 0.03 |
| $10^{13}$ | 395785.77 | 1278.31 | 0.0032 | 1.59 | 2.16 | 0.37 | 0.18 | 0.38 | 0.14 |
| $10^{14}$ | 396322.50 | 1815.04 | 0.0046 | 1.42 | 2.00 | 0.54 | 0.27 | 0.54 | 0.21 |

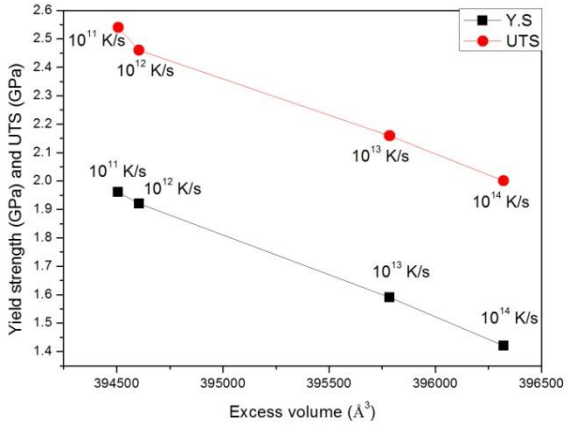


(a)

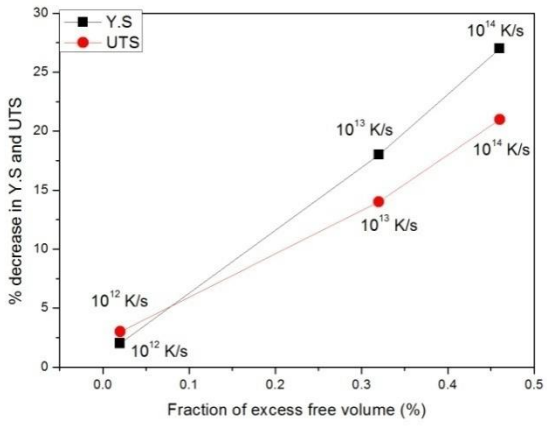


(b)

Fig.4.13: Shows excess free volume changes with yield strength and ultimate tensile strength.

### 4.2.5 Stress analysis

In Fig 4.14, during tensile deformation, we can detect that at 20% strain the maximum stress value is found to be 0.7125-0.7750 GPa, successively with increase in strain, the model alloy is deforming and at 50% and 80% necking can be witnessed and finally at 100% strain, the model alloy has been deformed.

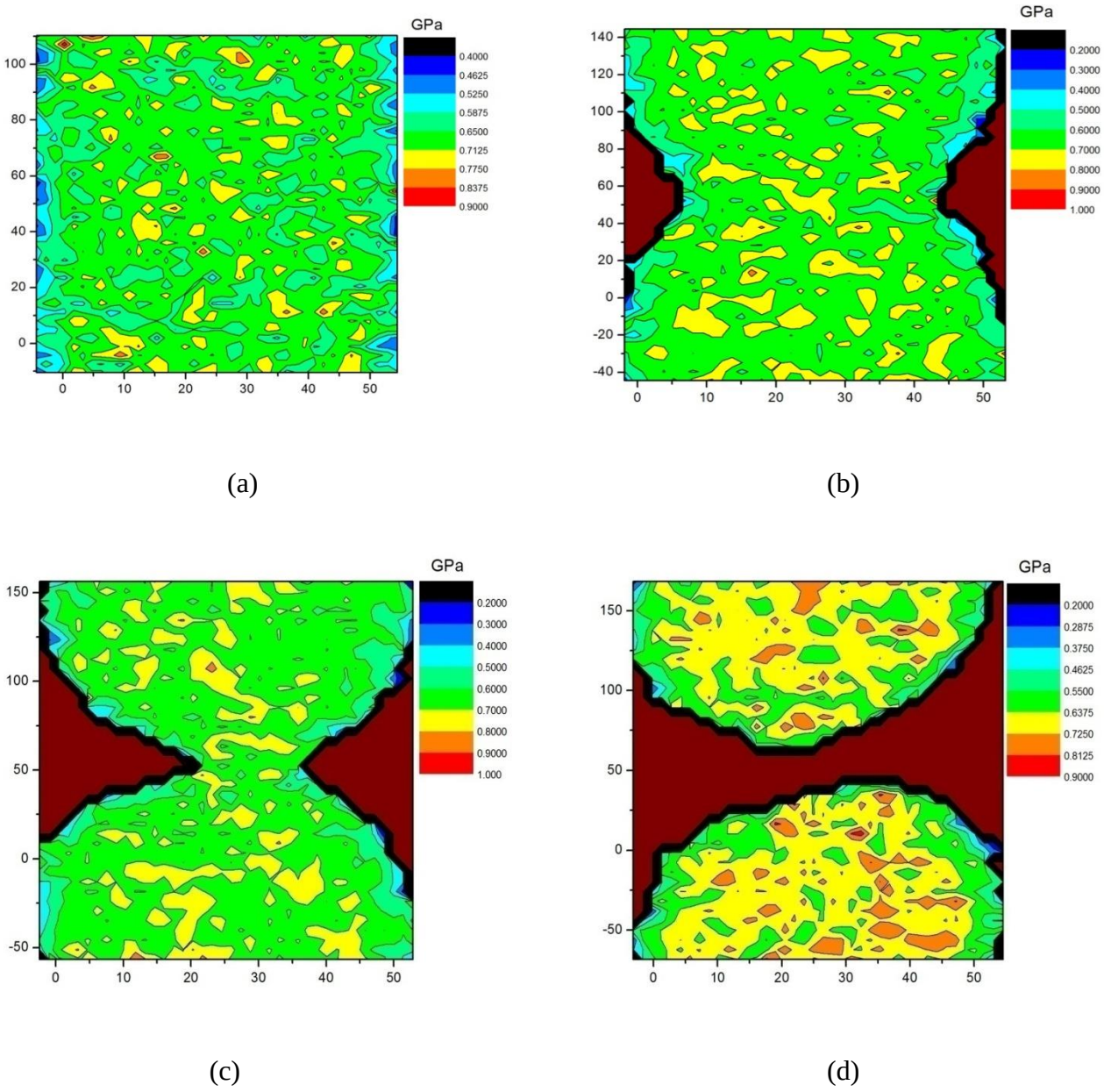


Fig 4.14: Contour plots at different strain values representing stress variation during tensile deformation: (a) 20% (b) 80% (c) 100% and (d) 140%.

### 4.3Compressive deformation of quenched specimen

After the development of glassy model alloy, uniaxial compressive deformation has been done at distinctive temperatures viz. 300K, 200K, 100K, 50K and 10K and strain rates viz. $1\times10^{8}s^{-1}$, $1\times10^{09}s^{-1}$, $1\times10^{10}s^{-1}$ and $1\times10^{11}s^{-1}$, in order to study the effect oftemperatures and strain rates on the model alloy. After compressive test, mechanical properties such as young's modulusand yield strength has been evaluated.

- This program is for obtaining compressive behavior of $Cu_{50}$-$Zr_{50}$ for 3D system ($10^{8}$ $s^{-1}$ strain rate).

```
Units           metal
echo            both
atom_style      atomic
dimension       3
boundary        s p s

read_data       CuZr_cooling_10_13.txt

timestep        0.002
pair_style      eam/fs
pair_coeff      * * CuZr_mm.eam.fs Cu Zr

# Energy Minimization

minimize        1.0e-9 1.0e-6 1000 1000

fix             A all nvt temp 300 300 0.1
run             10000


compute         1 all  stress/atom

compute         csym all centro/atom fcc
compute         peratom all pe/atom

variable        tmp equal ly
variable        lo equal ${tmp}
variable        strain equal (ly-v_lo)/v_lo


variable        p1 equal "-pxx/10000"
variable        p2 equal "-pyy/10000"
variable        p3 equal "-pzz/10000"
```

```
variable        p12 equal "-pxy/10000"
variable        p23 equal "-pyz/10000"
variable        p13 equal "-pxz/10000"


variable        fm equal "(v_p2+v_p3+v_p1)/3" ##### Hydrostatic stress

variable        fv equal "sqrt(((v_p2-v_p3)^2+(v_p3-v_p1)^2+(v_p1-
v_p2)^2+6*(v_p12^2+v_p23^2+v_p13^2))/2)" ######Von Mises Stress

variable        t equal "v_fm/v_fv"

variable        fd equal (((v_p2-v_fm)*(v_p3-v_fm)*(v_p1-v_fm))-(v_p12)^2*(v_p3-
                v_fm)-(v_p13)^2*(v_p2-v_fm)-(v_p23)^2*(v_p1-
                v_fm)+2*v_p12*v_p23*v_p13)####Deviatoric Von Mises stress

# principal stresses

variable        I1 equal "(v_p1+v_p2+v_p3)"

variable        I2 equal "((v_p1)*(v_p2))+((v_p2)*(v_p3))+((v_p1)*(v_p3))-(v_p12)^2-
                (v_p23)^2-(v_p13)^2"

variable        I3 equal "((v_p1)*(v_p2)*(v_p3))-((v_p1)*((v_p23)^2))-
            ((v_p2)*((v_p13)^2))-((v_p3)*((v_p12)^2))+2*(v_p12)*(v_p23)*(v_p13)"

variable        A equal "(acos(((2*(v_I1)^3)-9*(v_I1)*(v_I2)+27*(v_I3))/(2*((v_I1)^2-
                (3*(v_I2)))^(3/2))))/3"

variable        s1 equal "((v_I1)/3)+(2/3)*(sqrt((v_I1)^2-(3*(v_I2))))*cos(v_A)"

variable        s2 equal "((v_I1)/3)+(2/3)*(sqrt((v_I1)^2-
                (3*(v_I2))))*cos((v_A)+(2*PI)/3)"

variable        s3 equal "((v_I1)/3)+(2/3)*(sqrt((v_I1)^2-
(3*(v_I2))))*cos((v_A)+(4*PI)/3)"


thermo          10000
thermo_style    custom step temp  vol press pekeetotal

dump            1 all custom 10000 compression_CuZr.lammpstrj id type x  y z
dump            2 all cfg 10000 dump.compress_CuZr*.cfg mass type
xsyszsc_csymc_peratom

dump            3 all custom 10000 stress_peratom* id type x y z c_1[1] c_1[2] c_1[3]
c_1[4] c_1[5] c_1[6]
```

```
log             NVTlog5050_compress_CuZr.data
velocity        all create 300 873847 rot yes mom yes dist gaussian

# temperature controller

fix             1 all nvt temp 300 300 0.1

# tensile deformation

fix             2 all deform 1  y erate -0.0001  units box

fix             3 all print 10000 "${strain} ${p2}" file stress_strain_data.txt

fix             def all print 1 "${strain} ${p2} ${s1} ${s2} ${s3} ${fm} ${fv} ${t}
${fd}" file CuZr_compression_von.txt


run             1000000
```

### 4.3.1 Effect of strain rates

Fig.4.15, showsthe compressive deformation of various stress vs strain plots of $Cu_{50}$-$Zr_{50}$ model alloy at different strain rates in the range of $10^{08}s^{-1}$ -$10^{11}s^{-1}$ and temperatures viz. 300K, 200K, 100K, 50K and 10K. From figure, it has been shown that with varying strain rate the value of stress varies significantly.

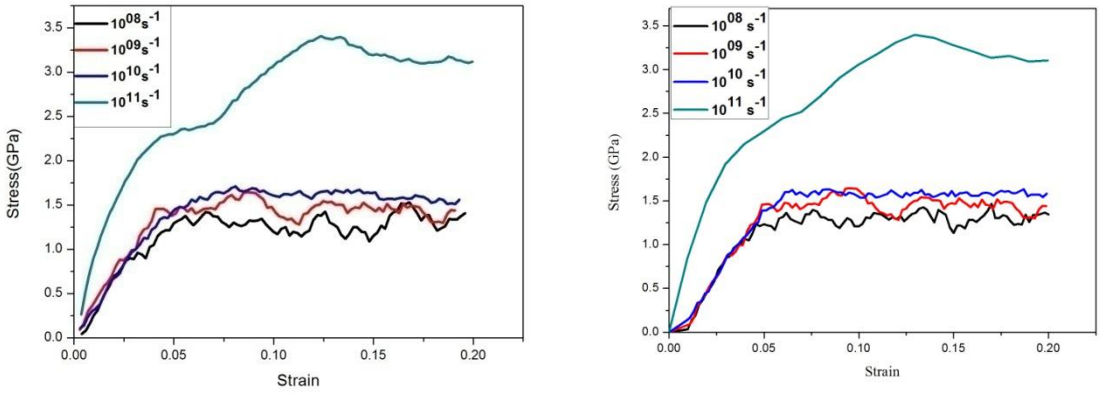


(a) (b)

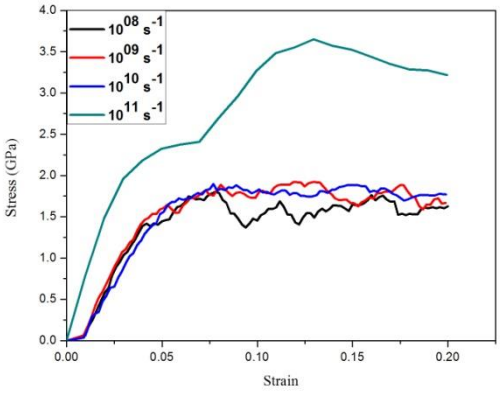


(c)

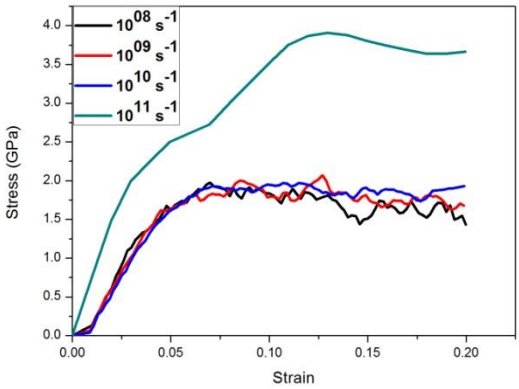


(d)

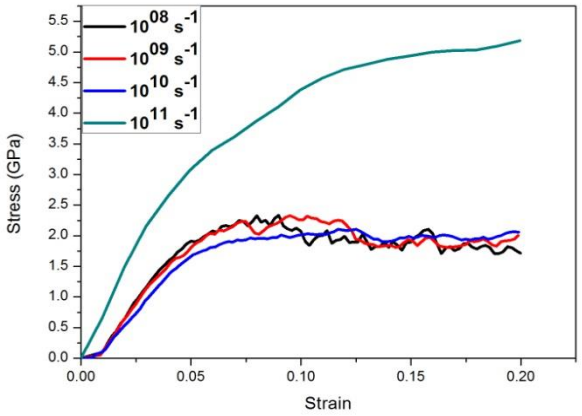


(e)

Fig. 4.15: Shows variation ofstrain rates ($10^{8}$ $s^{-1}$– $10^{11}$ $s^{-1}$) of model alloy at different temperatures (a) 300K (b) 200K (c) 100K (d) 50K (e) 10K.

### 4.3.1.1 Yield strength analysis

The simulation results focused on the effect of yield strength on $Cu_{50}$-$Zr_{50}$ model alloy at different strain rates, which are arranged in Table 4.6. From Table 4.6,it has been shown that theYield Strength significantlyvaries w.r.t different strain rates. The value of yield strength at$10^{8}$ $s^{-1}$ strain rate at room temperature is found to be 0.87GPa but in higher strain rate ($10^{11}$ $s^{-1}$ ) yield strength value is achieved 1.37GPa and simultaneously with varying temperatures, the yield strength value also varies.

The effect of different strain rate on yield strength of $Cu_{50}$-$Zr_{50}$alloy is depicted in Fig.4.16.

Table 4.6:Yield strength variation w.r.t different strain rate of $Cu_{50}$-$Zr_{50}$ model alloy.

| Model Alloy | Strain Rate ($ps^{-1}$) | Yield Stregth(GPa) (300K) | Yield Stregth(GPa) (200K) | Yield Stregth(GPa) (100K) | Yield Stregth(GPa) (50K) | Yield Stregth(GPa) (10K) |
|---|---|---|---|---|---|---|
| $Cu_{50}$-$Zr_{50}$ | 0.0001 | 0.87 | 0.47 | 1.38 | 1.28 | 1.18 |
| | 0.001 | 0.88 | 0.89 | 1.10 | 0.60 | 1.57 |
| | 0.01 | 1.35 | 1.42 | 0.35 | 0.69 | 1.42 |
| | 0.1 | 1.37 | 1.43 | 1.60 | 1.84 | 2.10 |

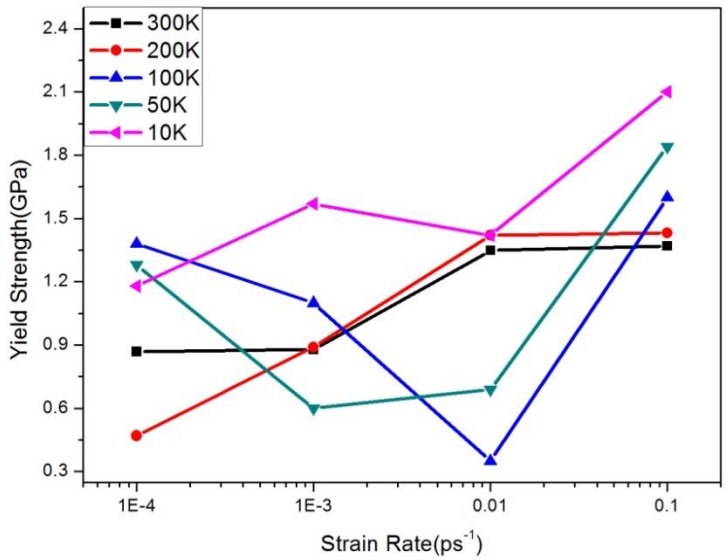


Fig 4.16:Yield strength vs strain rate plots.

### 4.3.1.2 Young's Modulus analysis

The simulation results focused on the effect of young's modulus on $Cu_{50}$-$Zr_{50}$ model alloy at different strain rates, which are arranged in Table 4.7. From Table 4.7, it has been shown that theyoung's modulus significantlyvaries w.r.t different strain rates. The value of

young's modulus at$10^8 s^{-1}$ strain rate at room temperature is found to be 34.16 GPa but in higher strain rate ($10^{11}$ $s^{-1}$) the value is achieved 49.92 GPa and simultaneously with varying temperatures, the young's modulus value also varies. The effect of different strain rate on yield strength of $Cu_{50}$-$Zr_{50}$alloy is depicted in Fig.4.17.

Table 4.7:Young's modulus variation w.r.t different strain rate of $Cu_{50}$-$Zr_{50}$ model alloy.

| Model Alloy | Strain Rate ($ps^{-1}$) | Young's Modulus (GPa) (300K) | Young's Modulus (GPa) (200K) | Young's Modulus (GPa) (100K) | Young's Modulus (GPa) (50K) | Young's Modulus (GPa) (10K) |
|---|---|---|---|---|---|---|
| $Cu_{50}$-$Zr_{50}$ | 0.0001 | 34.16 | 31.87 | 39.67 | 38.74 | 44.25 |
| | 0.001 | 38.42 | 31.55 | 36.50 | 39.63 | 33.69 |
| | 0.01 | 32.71 | 30.06 | 33.52 | 34.74 | 37.84 |
| | 0.1 | 49.92 | 54.15 | 66.51 | 67.82 | 68.43 |

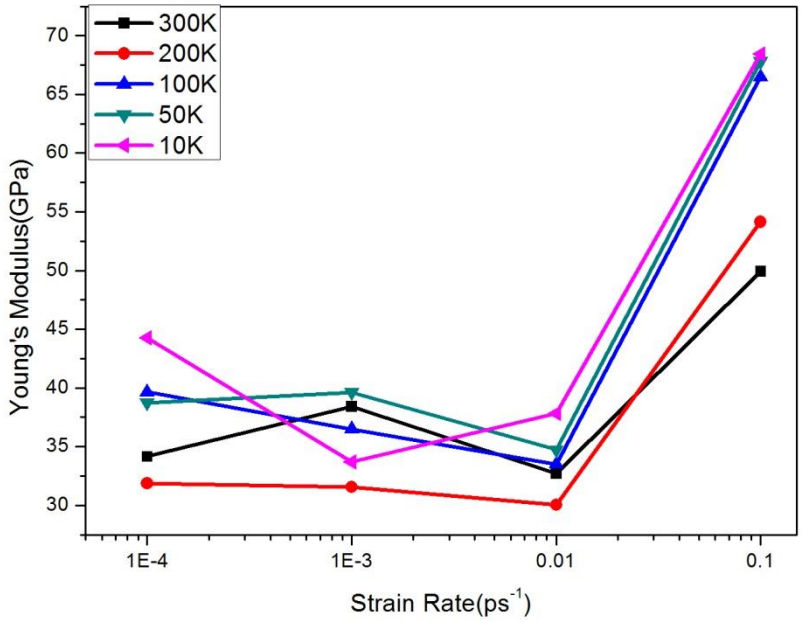


Fig.4.17: Young's modulus vs strain rate plots.

### 4.3.2 Effect of temperatures

Fig.4.18, showsthe compressive deformation of various stress vs strain plots of $Cu_{50}$-$Zr_{50}$ model alloy at two strain rates$10^{8}s^{-1}$and $10^{11}s^{-1}$ and temperatures viz. 300K, 200K, 100K, 50K and 10K. From figure, it has been shown that with decreasingtemperatures the value of stress increases significantly.

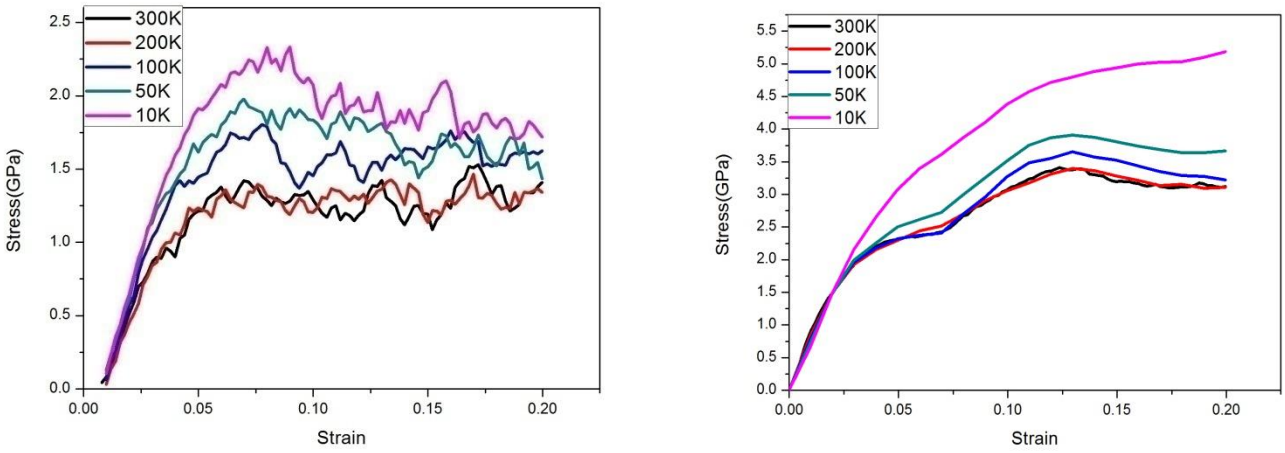


Fig.4.18:Shows variation oftemperatures of model alloy at strain rates (a) $10^{8}$ $s^{-1}$ (b) $10^{11}$ $s^{-1}$.

#### 4.3.2.1 Yield strength variation

The simulation results focused on effect of yield strength on $Cu_{50}$-$Zr_{50}$ model alloy at different temperatures, which are arranged in Table 4.8. From Table 4.8, it has been shown that the yield strength significantlyvaries w.r.t different temperatures. At room temperature the value of yield strength is found to be 0.87 GPa but in lower temperature(10K) the value is found to be 1.18 GPa and simultaneously with varying strain rates, the yield strength value also varies. The effect of different temperatures on yield strength of $Cu_{50}$-$Zr_{50}$alloy is depicted in Fig.4.19.

Table 4.8:Yield strength variation w.r.t different strain rate of $Cu_{50}$-$Zr_{50}$ model alloy.

| Model Alloy | Temperatures (K) | Yield Strength(GPa) (0.0001 $ps^{-1}$) | Yield Strength(GPa) (0.001 $ps^{-1}$) | Yield Strength(GPa) (0.01 $ps^{-1}$) | Yield Strength(GPa) (0.1 $ps^{-1}$) |
|---|---|---|---|---|---|
| $Cu_{50}$-$Zr_{50}$ | 300 | 0.87 | 0.88 | 1.35 | 1.37 |
| | 200 | 0.47 | 0.89 | 1.42 | 1.43 |
| | 100 | 1.38 | 1.10 | 0.35 | 1.60 |
| | 50 | 1.28 | 0.60 | 0.69 | 1.84 |
| | 10 | 1.18 | 1.57 | 1.42 | 2.10 |

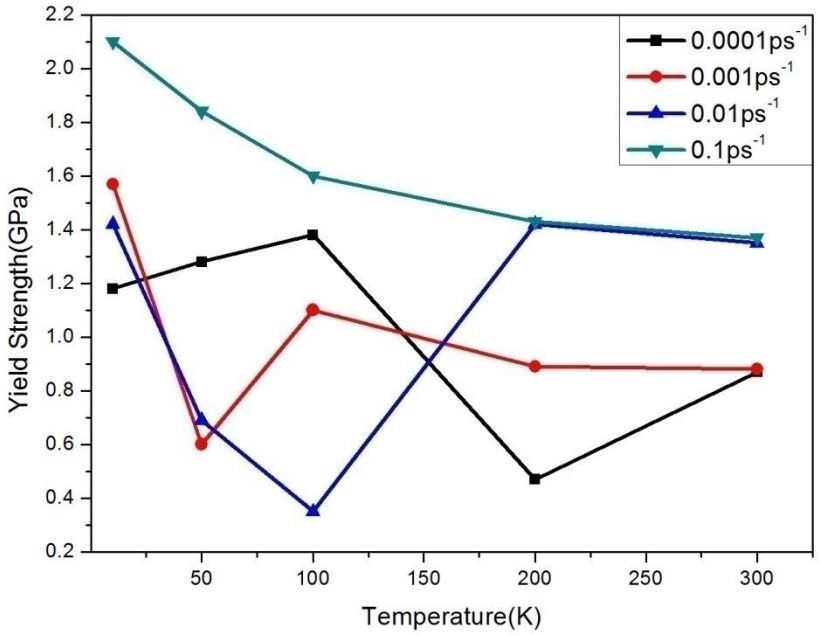


Fig 4.19: Yield strength vs. Temperature plots.

### 4.3.2.2 Young's modulus variation

The simulation results focused on the effect of young's modulus on $Cu_{50}$-$Zr_{50}$ model alloy at different temperatures, which are arranged in Table 4.9. From Table 4.9, it has been shown that theyoung's modulus significantlyvaries w.r.t different temperatures. The value of young's modulus at room temperature is found to be 34.16 GPa but atlow temperature (10 K)the value is achieved 44.25 GPa and simultaneously with varying temperatures, the value of young's modulus also varies.

The effect of different temperatureson young's modulus of $Cu_{50}$-$Zr_{50}$alloy is depicted in Fig.4.20.

Table 4.9: Young's modulus variation w.r.t different temperatures of $Cu_{50}$-$Zr_{50}$ model alloy.

| Model Alloy | Temperatures (K) | Young's Modulus (GPa) ($0.0001\ ps^{-1}$) | Young's Modulus (GPa) ($0.001\ ps^{-1}$) | Young's Modulus (GPa) ($0.01\ ps^{-1}$) | Young's Modulus (GPa) ($0.1\ ps^{-1}$) |
|---|---|---|---|---|---|
| $Cu_{50}$-$Zr_{50}$ | 300 | 34.16 | 38.42 | 32.71 | 49.92 |
| | 200 | 31.87 | 31.55 | 30.06 | 54.15 |
| | 100 | 39.67 | 36.50 | 33.52 | 66.51 |
| | 50 | 38.74 | 39.63 | 34.74 | 67.82 |
| | 10 | 44.25 | 33.69 | 37.84 | 68.43 |

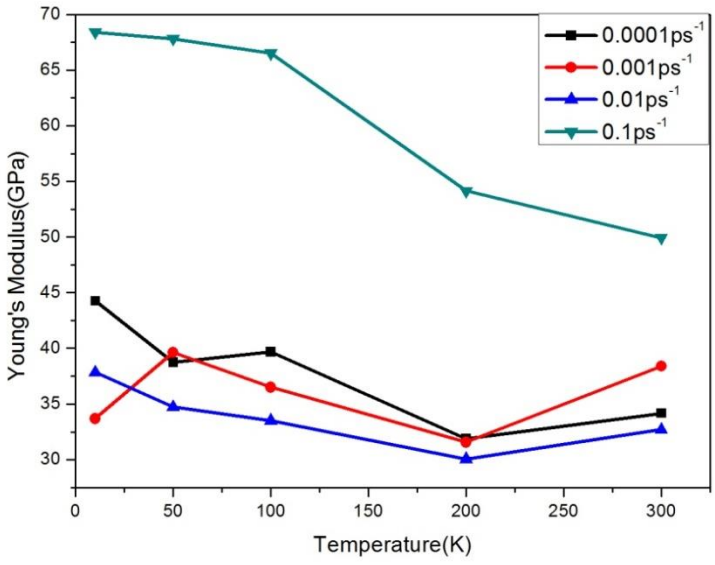


Fig 4.20: Young's modulus vs Temperature plots.

# CHAPTER-5

# CONCLUSIONS

# 5 CONCLUSIONS

a) $Cu_{50}$-$Zr_{50}$ glassy samples are obtained at different cooling rates in the range of $10^{10}$ K/s - $10^{14}$ K/s. The sample with the highest cooling rate has 1815.04 $Å^3$ excess free volume.

b) MD simulation suggest that the cooling rate has significant effect on the nature of the stress-strain behaviour and also on the mechanical properties of $Cu_{50}$-$Zr_{50}$ glassy samples.

c) The $Cu_{50}$-$Zr_{50}$glassy sample with excess free volume yields at much lower stress compared to the other samples at all strain rates and temperatures.

d) Yield strength increases with increase strain rate and decrease of temperature.

e) The stress contours of tensile samples show high magnitude of stress in the regions close to the necking.

# CHAPTER-6

# REFERENCES

# 6 REFERENCES

[1] P. Duwez, F. H. Brown Jun. and F. Odell, the Zirconia -Yttria System, J. Electrochem. Soc.1951, 98: 356.

[2] Lee, S. W., Huh, M. Y., Fleury, E., Lee, J. C. (2006), Crystallization-induced plasticity of Cu-Zr containing bulk amorphous alloys, ActaMaterialia, Vol. 54, No. 2, pp. 349-355.

[3] Mattern, N., Bednarcik, J., Pauly, S., Wang, G., Das, J., Eckert, J. (2009), Structural evolution of Cu-Zr metallic glasses under tension, actaMaterialia, Vol. 57, No. 14, pp. 4133-4139.

[4] Wei, X. F., Sun, Y. F., Guan, S. K., Terada, D., Shek, C. H. (2009), Compressive and tensile properties of Cu-Zr alloy plates containing martensitic phases, Materials Science and Engineering, Vol. 517, No. 1-2, pp. 375-380.

[5] Xue, Y. F., Cai, H. N., Wang, L., Wang, F. C., Zhang, H. F. (2008), Effect of loading rate on failure in Zr-based bulk metallic glass, Materials Science and Engineering, Vol. 473, No. 1-2, pp. 105-110.

[6] Pauly, S., Das, J., Duhamel, C., Eckert, J. (2007), Martensite Formation in a Ductile $Cu_{47.5}Zr_{47.5}Al_5$ Bulk Metallic Glass Composite, Advanced Engineering Materials, Vol. 9,No. 6, pp. 487-491.

[7] Mondal, K., Ohkubo, T., Toyama, T., Nagai, Y., Hasegawa, M., Hono, K. (2008), The effect of nanocrystallization and free volume on the room temperature plasticity of Zr-based bulk metallic glasses, ActaMaterialia, Vol. 56, No. 18, pp. 5329-5339.

[8] Pauly, S., Das, J., Duhamel, C., Eckert, J. (2008), Effect of Titanium on Microstructure and Mechanical Properties of $Cu50Zr50- x$ Ti $x$ ($2.5 \leq x \leq 7.5$) Glass Matrix Composites, Metallurgical and Materials Transactions A, Vol. 39, No. 8, pp. 1868-1873.

[9] Yu, P., Bai, H. Y. (2008), Poisson's ratio and plasticity in CuZrAl bulk metallic glasses, Materials Science and Engineering A, Vol. 485, No. 1-2, pp. 1-4.

[10] Das, J., Tang, M. B., Kim, K. B., Theissmann, R., Baier, F., Wang, W. H., Eckert, J. (2005) "Work-Hardenable" Ductile Bulk Metallic Glass, Physical Review Letters, Vol. 94, No. 20, pp. 205-501.

[11] Lavernia, E. J., Srivatsan, T. S. (2010), The rapid solidification processing of materials: scscience, principles, technology, advances, and applications, Journal of Materials Science, Vol. 45, No. 2, pp. 287-325.

[12] Suryanarayana, C., Inoue A. (2010), Bulk Metallic Glasses, Florida, CRC press.

[13] Anantharaman, T. R. (1984), Metallic glasses: production, properties and applications, Switzerland, Trans Tech publications, First Edition.

[14] Inoue, A., Nishiyama, N. (1997), Extremely low critical cooling rates of new Pd-Cu-P base base amorphous alloys, Materials Science and Engineering A, Vol. 226, pp. 401-405.

[15] Peker, A., Johnson, W. L. (1993), A Highly Processable Metallic-Glass-$Zr_{41.2}Ti_{13.8}Cu_{12.5}$ Ni10.0Be22.5, Applied Physics Letters, Vol. 63, No. 17, pp. 2342-2344.

[16] Hajime Tanaka, Relationship among glass-forming ability, fragility, and short-range bond ordering of liquids, Journal of Non-Crystalline Solids. 2005, 351: pp.678–690.

[17] MEI Jinna, Titanium-based Bulk Metallic Glasses: Glass Forming Ability and Mechanical Behaviour, PhD Thesis, Joseph Fourier University – Grenoble North-western Polytechnic University.

[18] Moynihan, The Glass Transition and the Nature of the Glassy State, Ann. NY Acad. Sci. 1976, 279: 15–36.

[19] Brüning, R. &Samwer, Glass transition on long time scales, Phys. Rev. 1992, 46, pp.318–322.

[20] H S Chen, Glassy metals, Rep. Prog. Phys. 1980, 43.

[21] Christopher A. Schuh, Todd C. Hufnagel b, UpadrastaRamamurty, Mechanical behaviour of amorphous alloys, ActaMaterialia. 2007, 55: pp. 4067–4109.

[22] Trexler, Thadhani, Mechanical properties of bulk metallic glasses, Prog Mater Sci. 2010, 55: 759-836.

[23] Y. Wua, H. Wang , H.H. Wua, Z.Y. Zhang , X.D. Hui , G.L. Chen , D. Ma, X.L. Wang , Z.P. Lu, Formation of Cu–Zr–Al bulk metallic glass composites with improved tensile properties, ActaMaterialia. 2011, 59: pp. 2928–2936.

[24] Hofmann DC, Suh JY, Wiest A, Duan G, Lind ML, Demetrious MD, Nature. 2008, 451:1085.

[25] Hofmann DC, Suh JY, Wiest A, Lind ML, Demetriou MD, Johnson WL. ProcNatlAcadSci, USA. 2008, 105: 20136.

[26] N.S. Barekara, S. Paulya, R.B. Kumarb, U. Kühna, B.K. Dhindawc, J. Eckerta, Structure–property relations in bulk metallic Cu–Zr–Al alloys, Materials Science and Engineering A. 2010, 527: 5867–5872.

[27] Hirata, A., Guan, P. F., Fujita, T., Hirotsu, Y., Inoue, A., Yavari, A. R., Sakurai, T., Chen,M. W.(2011), Direct observation of local atomic order in a metallic glass, Nature Materials, Vol. 10, No. 1, pp. 28-33.

[28] Kramer, M. J., Besser, M. F., Rozhkova, E., Sordelet, D. J. (2004), Influence of short rangeorder on devitrification in Zr70Pd20Cu10metallic glasses, Intermetallics, Vol.12, No. 10-11, pp. 1119-1124.

[29] Miracle, D. B. (2004), A structural model for metallic glasses, Nature Materials, Vol. 3, No.10, pp. 697-702.

[30] Turnbull, D., Cohen, M.H., (1960), Crystallization kinetics and glass formation, in: Modern Aspects of the Vitreous State, Ed. Mackenzie, J. D., London: Butterworth, First Edition, pp. 38-62.

[31] Turnbull, D., Cohen, M. H. (1970), On the Free-Volume Model of the Liquid-Glass Transition, The Journal of Chemical Physics, Vol. 52, No. 6, pp. 3038-3041.

[32] Argon, Plastic Deformation in Metallic glasses, ActaMaterialia. 27: 47-58.

[33] Spaepen F, A microscopic mechanism for steady state inhomogeneous flow in metallic glasses, ActaMaterialia. 1977, 25: 407-415

[34] Morrel H. Cohen and David Turnbull, Molecular Transport in Liquids and Glasses, Journal of Chemical Physics. 1959, 31: 1164-1169.

[35] Nieh, Wadsworth, Homogeneous behavior of bulk metallic glasses, ScriptaMaterialia. 2006, 54: 387–392.

[36] Y. Kawamura, T. Nakamura, A. Inoue, Superplasticity in Pd40Ni40P20 Metallic Glass, Scripta Mater. 1998, 39: 301–306.

[37] V.A. Khonik, V.A. Zelenskiy, High- temperature ductility and superplasticity of metallic glasses ,Phys Met Metall. 1989, 67: 196-201.

[38] W. H. Jiang, F. X. Liu, D. C. Qiao, H. Choo, P. K. Liaw, R. Li, and T. Zhang, Effects of Temperatures on Inhomogeneous Plastic Flows of a Bulk-Metallic Glass, Advanced Engineering Materials. 2008, 10: 11.

[39] Duhamel, C., Das, J., Pauly, S., Lee, K. S., Eckert, J. (2008), Deformation behaviour and fractrographic features of ductile $Cu_{47}Zr_{47}Al_6$ bulk metallic glass, Reviews on Advanced Materials Science, Vol. 18, No. 6, pp. 527-533.

[40] Hajlaoui, K., Stoica, M., LeMoulec, A., Chariot, F., Yavari, A. R. (2008), Strain rate effect on deformation of Zr-based metallic glass: In-situ tensile deformation in sem analysis, Reviews on Advanced Materials Science, Vol. 18, No. 1, pp. 23-26.

[41] Ge, Y. N., Song, W. B., Wang, X. F., Luo, Z. C., Li, W., Lin, J. G. (2010), Temperatures and strain rate dependence of deformation behavior of Zr65Al7.5Ni10Cu17.5,Materials Chemistryand Physics, Vol. 124, No. 1, pp. 25-28.

[42] Launey, M.E., Busch, R., Kruzic, J. J., (2008), Effects of free volume changes and residual stresses on the fatigue and fracture behaviour of a Zr-Ti-Ni-Cu-Be bulk metallic glass, ActaMaterialia, 56, 500-510.